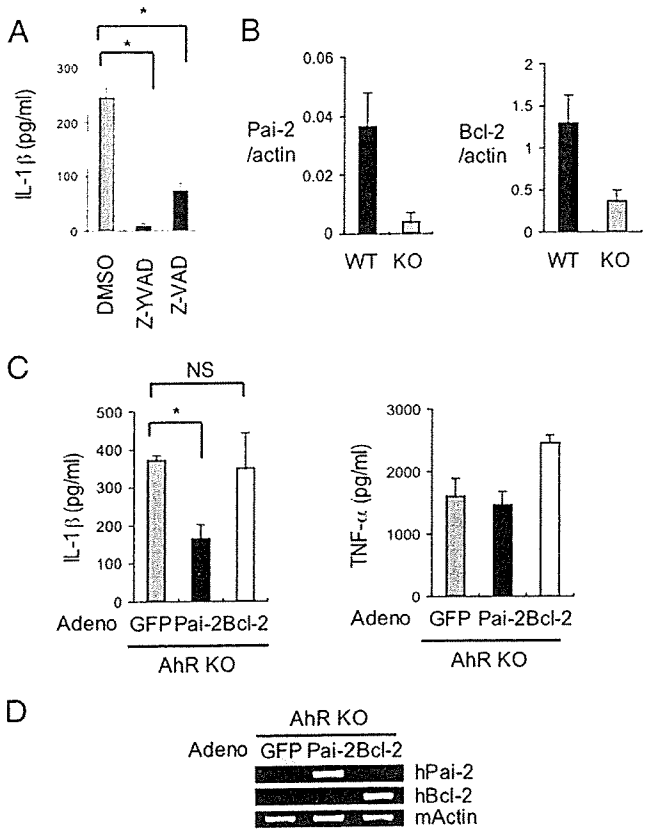

FIG. 3. Decreased Pai-2 expression is one of the causes of the increased IL-1β secretion by LPS-treated AhR KO BMDM. (A) Inhibition of IL-1β oversecretion from AhR KO BMDM by treatment with caspase-1 inhibitor (Z-YVAD-FMK) or caspase inhibitor (Z-VAD-FMK). (B) Relative expression levels of Pai-2 and Bcl-2 mRNA in AhR WT and AhR KO BMDM. (C) The effect of hPai-2 and hBcl-2 reconstitution on the LPS-induced secretion of IL-1β and TNF-α by AhR KO BMDM. BMDM from AhR KO mice were infected with the individual adenovirus (adeno) vectors and then washed and incubated for 24 h. IL-1β and TNF-α levels in the supernatants 8 h after LPS stimulation (n = 3) were determined by ELISA. (D) Assessment of hPai-2 and hBcl-2 mRNA expression in adenovirus (adeno) vector-infected BMDM by conventional RT-PCR. Error bars show standard deviations. *, $P < 0.001$; NS, not significant.

stream of the transcription start site, we were interested in determining whether Arnt was also involved in the inducible expression of Pai-2 by LPS. Other AhR target genes identified by the microarray analysis, e.g., the matrix metalloproteinase (Mmp-8) gene and the NAD(P)H:quinone oxidoreductase 1 (Nqo1) gene (Table 1), have characteristic XRE sequences in their promoter regions and were also induced by 3MC. As expected, the induction of their expression was greatly reduced in Arnt KO and Arnt small interfering RNA (siRNA)-treated macrophages (Fig. 4E; also see Fig. S1 in the supplemental material). In stark contrast, the expression of Pai-2 was not much different in Arnt KO and Arnt siRNA-treated macrophages, indicating that Arnt is not involved in regulating Pai-2 gene expression (Fig. 4D; also see Fig. S1 in the supplemental material) and that AhR regulates Pai-2 gene expression by a noncanonical mechanism. Consistent with these observations, macrophage-specific conditional deletion of Arnt did not significantly alter the sensitivity to LPS treatment (Fig. 4F).

DNA elements regulating Pai-2 gene expression. We were interested in further investigating how AhR regulates Pai-2 gene expression in macrophages. It has been previously reported that LPS-induced Pai-2 expression requires NF-κB activation (21) and that AhR and p65 physically interact with each other (31). With those results in mind, we constructed a reporter gene by fusing a 2.7-kb sequence upstream of the mouse Pai-2 transcription start site to the luciferase gene (see Fig. S2 in the supplemental material). This 2.7-kb Pai-2 reporter gene contained a previously reported NF-κB site (21). When the AhR expression vector alone was transfected into RAW 264.7 cells, it did not enhance LPS-induced reporter gene expression. In contrast, cotransfection of both AhR and p65 did (Fig. 5A). To identify the sequence responsible for enhancing the LPS-induced activation of the reporter gene, we constructed an 0.8-kb Pai-2 reporter gene by deleting the sequence from −2.7 to −0.8 kb, which contained the previously reported NF-κB site (see Fig. S2 in the supplemental material). With this 0.8-kb Pai-2 construct, the addition of AhR and p65 no longer enhanced the activity in response to LPS treatment (Fig. 5A), indicating that the sequence between −0.8 and −2.7 kb, containing an NF-κB site, is responsible for enhancing Pai-2 gene activation in response to AhR and NF-κB. Further downstream, we noticed the presence of a putative C/EBPβ binding sequence (around 250 base pairs upstream of the transcription initiation site), which has been reported to be responsible for LPS-induced activation of the gene (4). Deletion or point mutation of this sequence was found to abrogate the ability of LPS to induce this gene, indicating that this C/EBPβ binding site functions as an enhancer sequence in the LPS response (see Fig. S2 in the supplemental material).

Recruitment of transcription factors necessary for LPS-induced Pai-2 expression. When macrophages were treated with LPS, p65 translocated from the cytoplasm into the nucleus independently of AhR (Fig. 5B), as reported previously. However, without AhR, ChIP revealed that p65 was not recruited to the enhancer sequence in the Pai-2 gene, which contains an NF-κB site (Fig. 5E). In WT macrophages, nuclear-translocated p65 was only recruited to the enhancer sequence of the Pai-2 gene together with AhR. PolII was concomitantly recruited to the TATA sequence of the Pai-2 gene in AhR WT but not AhR KO macrophages. Surprisingly, we observed that LPS induced AhR binding to the Pai-2 NF-κB site, as shown by ChIP using an anti-AhR antiserum. Co-IP assays revealed that AhR and p65 interacted in macrophages (Fig. 5C), consistent with a previous report (31). On the other hand, expression of the Cox-2 gene is known to be activated by LPS through recruitment of p65 to its NF-κB binding site, and this occurs independent of AhR (Fig. 5D), with concomitant binding of PolII to the transcription initiation site (TATA) of the Cox-2 gene (Fig. 5E). Arnt was not recruited to the Pai-2 promoter by ChIP assay (data not shown), consistent with normal Pai-2 expression in the macrophages from $Arnt^{flox/-}$::LysM Cre mice (Fig. 4D).

As shown in Fig. S3 in the supplemental material, the CCAAT box sequence in the Pai-2 gene was recognized by C/EBPβ in an LPS-dependent manner in both AhR WT and KO macrophages. This binding of C/EBPβ to the Pai-2 pro-

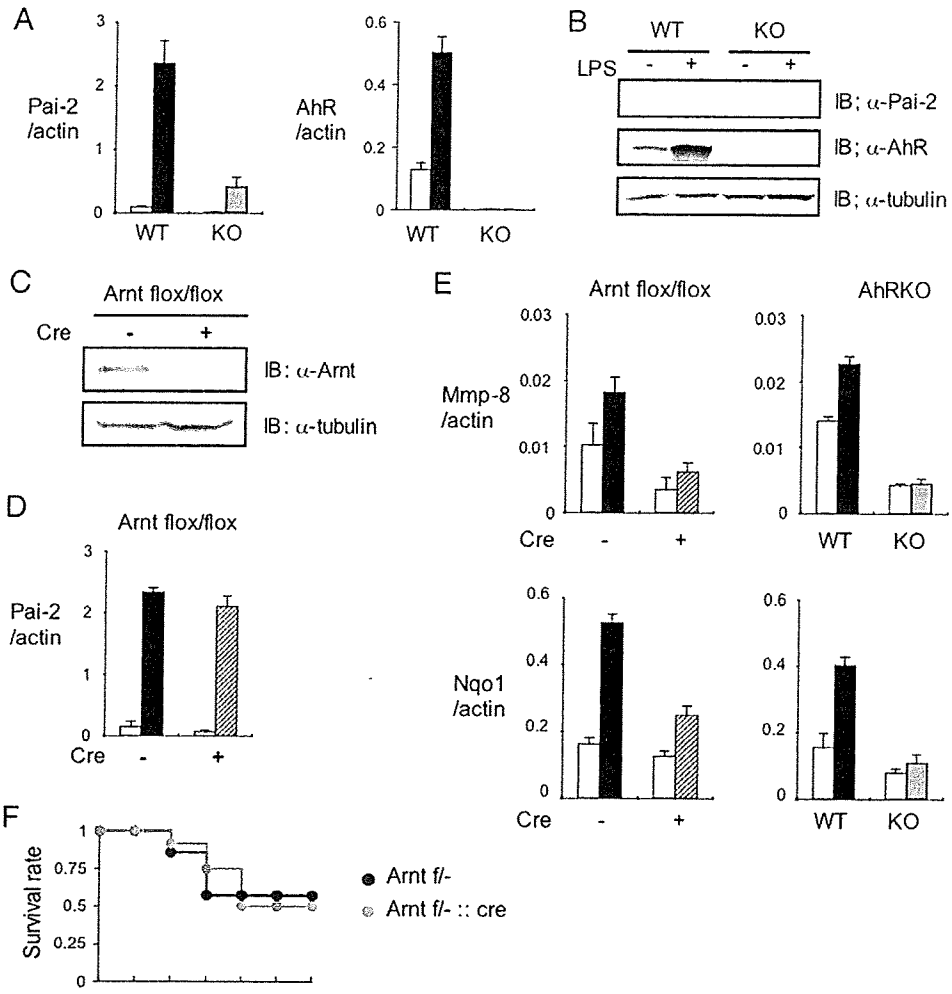

FIG. 4. Arnt is not required for LPS-induced enhancement of Pai-2 expression. (A) Relative Pai-2 and AhR mRNA expression levels in AhR WT and AhR KO PEMs 4 h after treatment with (black or gray bars) or without (white bars) LPS (10 ng/ml). (B) Immunoblot analysis of Pai-2 and AhR expression in AhR WT and KO PEMs after a 16-h incubation with LPS (10 ng/ml). (C) Immunoblot analysis of Arnt in $Arnt^{flox/flox}$ and $Arnt^{flox/flox}$::LysM Cre PEMs. (D) Relative Pai-2 mRNA expression levels 4 h after incubation of $Arnt^{flox/flox}$ (black bar) and $Arnt^{flox/flox}$::LysM Cre (hatched bar) PEMs with LPS (10 ng/ml). (E) Left, relative expression levels of Mmp-8 and Nqo1 mRNA in $Arnt^{flox/flox}$ (black bar) and $Arnt^{flox/flox}$::LysM Cre (hatched bar) PEMs treated with DMSO (white bars) or 3MC (black or hatched bar) (1 μM). Right, relative expression levels of Mmp-8 and Nqo1 mRNA in AhR WT (black bar) and AhR KO (gray bar) PEMs treated with DMSO (white bars) or 3MC (black or gray bar) (1 μM). (F) Survival of $Arnt^{flox/-}$ (Arnt f/−; n = 7) and $Arnt^{flox/-}$::LysM Cre (Arnt f/−::cre; n = 12) mice after LPS challenge (25 mg/ml). Error bars show standard deviations. IB, immunoblot; +, present; −, absent; α, anti.

moter might explain the weak LPS-induced activation of Pai-2 gene expression in AhR KO macrophages (Fig. 4A; also see Fig. S3 in the supplemental material), as described in the previous section.

The requirement of the functional domains of AhR for AhR-dependent Pai-2 expression. To determine the functional domains of AhR for AhR-dependent Pai-2 expression, we investigated the Pai-2 expression in ANA-1 cells, which were transfected with various AhR mutants (Fig. 6). Compared with the levels in ANA-1 cells transfected with full-length AhR, we observed much lower levels of expression of Pai-2 in the ANA-1 cells transfected with AhR NLSm (a mutant located predominantly in the cytoplasm) (Fig. 6B, bars 3, 4, 11, and 12). On the other hand, transfection with AhR CA (a constitutively active mutant located predominantly in the nucleus) gave a result for Pai-2 expression comparable to that of the transfection with full-length AhR (Fig. 6B, bars 3, 4, 7, and 8). These results indicated that nuclear AhR functions in AhR-dependent Pai-2 expression. The fractionation of AhR indicated that a small but significant amount of AhR existed in the nucleus without treatment with ligands such as 3MC, in contrast with the large amount in the cytoplasm (Fig. 5B), consistent with the previous report that AhR has functional nuclear localization signal and nuclear export signal sequences and shuttles between the cytoplasm and nucleus. It is reported that when nuclear export is inhibited by trichomycin B or phosphorylation at S68, AhR accumulates in the nucleus (12). Therefore, it could be considered that in macrophages, AhR is in-

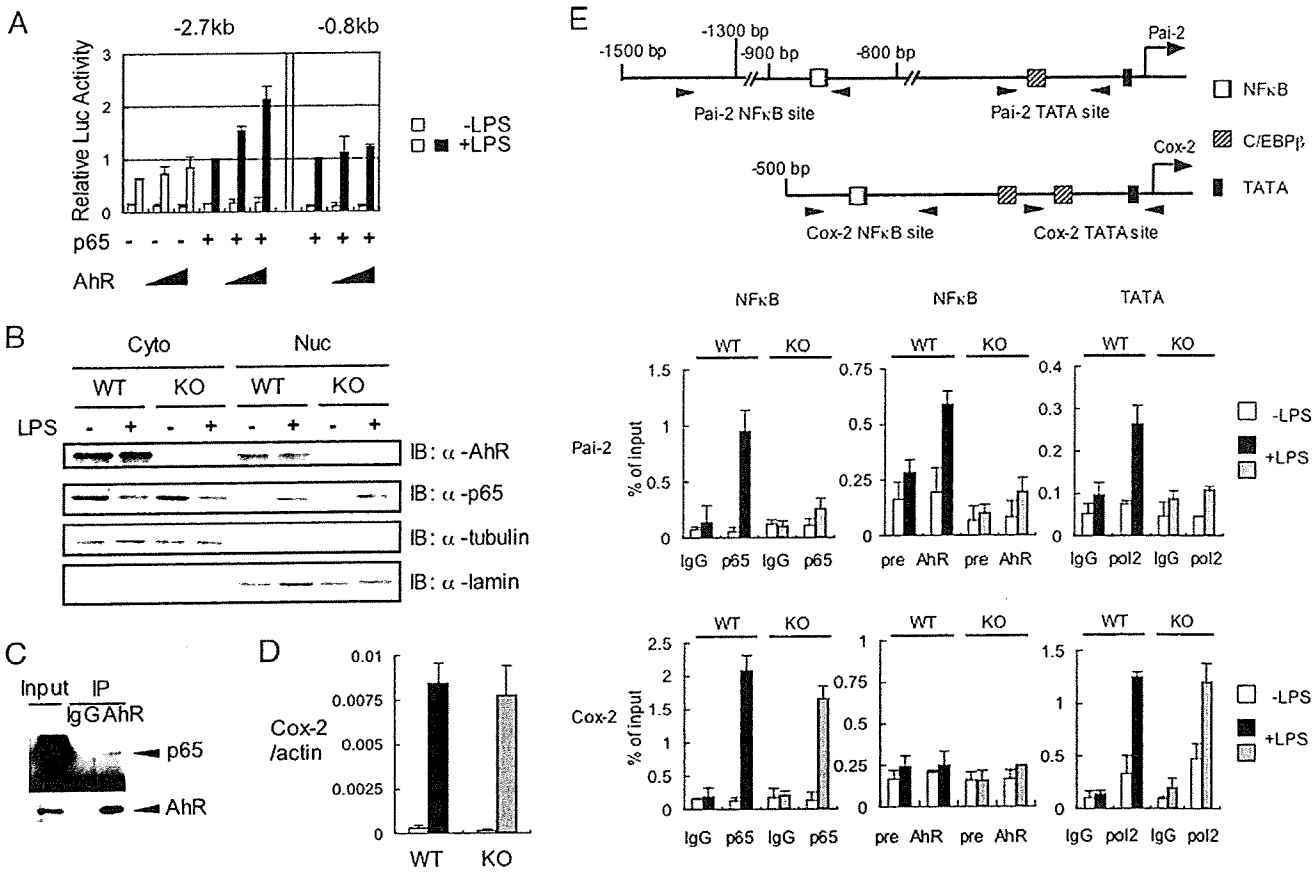

FIG. 5. Recruitment of transcription factors necessary for LPS-induced Pai-2 expression. (A) LPS-induced luciferase expression from the Pai-2 (−2.7 kb) and Pai-2 (−0.8 kb) reporter genes. RAW 264.7 cells were transfected with each reporter gene, with and without pcDNA3-AhR (0 ng, 50 ng, 100 ng) and/or pcDNA3-p65 (1 ng). Values represent the means, normalized to *Renilla* luciferase activity (used as an internal control), ± standard deviations of the results of three independent experiments. The activities shown by the fourth and seventh pairs of bars were used as standards for normalizing the relative activities of the other conditions. (B) AhR WT and AhR KO PEMs were left untreated or were treated with LPS for 1 h. Cytoplasmic (Cyto) and nuclear (Nuc) extracts were immunoblotted with antibodies against AhR, p65, tubulin, and lamin. (C) Co-IP of AhR and p65. Whole-cell extracts from AhR WT PEMs were coimmunoprecipitated with anti-AhR antibody. Co-IPs and Western blotting were performed as described in Materials and Methods. (D) Relative expression levels of Cox-2 mRNA in AhR WT and AhR KO PEMs after 4 h of treatment with or without LPS (10 ng/ml). Bars are as labeled in panel A. Error bars show standard deviations. (E) Top, transcription factor binding sites in the Pai-2 and Cox-2 genes. Bottom, results of ChIP analyses of the Pai-2 and Cox-2 promoters. ChIP analyses were performed using antibodies to p65, AhR, and PolII in LPS-induced AhR WT and AhR KO PEMs. ChIP analyses and real-time PCRs were performed as described in Materials and Methods. Error bars show standard deviations. +, present; −, absent; α, anti; IgG, immunoglobulin G.

volved in Pai-2 expression induced by LPS treatment in the absence of typical AhR ligands (Fig. 4A). The mechanism of AhR's involvement in Pai-2 expression induced by LPS will be investigated in detail. To further address the question of the requirement for the AhR domain in Pai-2 expression, we generated ANA-1 cells stably transfected with AhR ΔC (an activation domain-deficient mutant) and AhR Y9F (the mutant with attenuated DNA binding) (18). Compared with the expression in stable ANA-1 cells transfected with full-length AhR, neither of the cell lines transfected with AhR ΔC or AhR Y9F significantly expressed Pai-2 (Fig. 6B, bars 3 to 6, 9, and 10). These results indicate that both the activation and DNA binding domains of AhR were required for AhR-dependent Pai-2 expression. Co-IP analysis using these AhR mutants showed that the N-terminal region of AhR (AhR ΔC mutant) interacted with p65 (Fig. 6C).

DISCUSSION

AhR was originally found as a transcription factor that was involved in the induction of xenobiotic-metabolizing CYP1A1 by TCDD and other PAHs and has been found to act as a multifunctional regulatory factor in areas ranging from drug metabolism to innate immunity, providing protection against invading xenobiotics. Close investigation of the phenotypes of AhR KO mice revealed that they seem to suffer from morbidity from impaired immunity and easily succumb to bacterial infection. We examined the susceptibility of AhR KO mice to LPS-induced septic shock and found that they were hypersensitive to LPS treatment and had increased secretion of proinflammatory cytokines, such as IL-1β, TNF-α, IL-18, and IFN-γ (Fig. 1A and B). It has been reported that in endotoxic shock, IL-1β and TNF-α are rapidly released and trigger a secondary

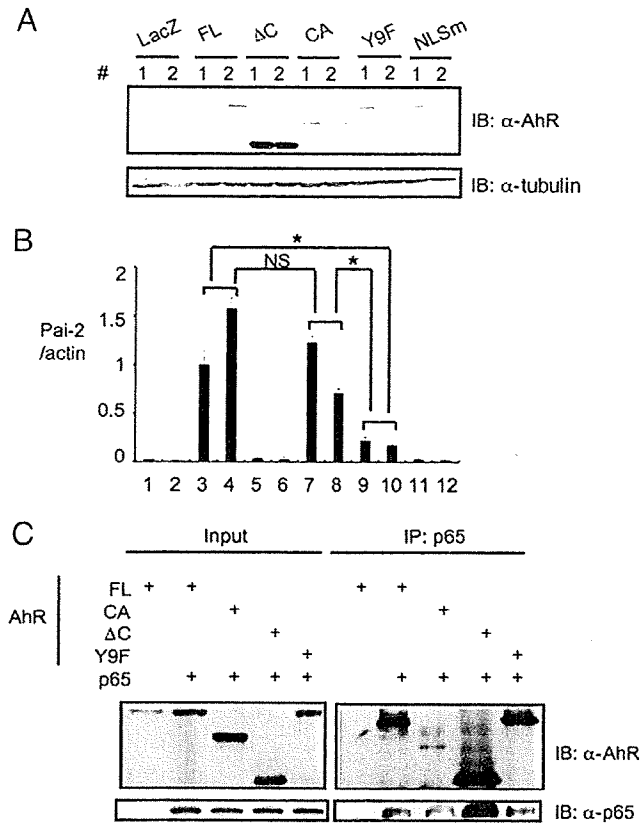

FIG. 6. Nuclear localization, activation, and DNA binding domains of AhR are required for AhR-dependent Pai-2 expression. (A) Immunoblot analysis of full-length AhR or mutants in LacZ or AhR transformant ANA-1 cells. Paired lanes labeled 1 and 2 show results from experiments using two independent transformants. (B) Relative expression levels of Pai-2 mRNA in ANA-1 cells transfected with LacZ or full-length AhR or mutants. Bars show quantification of the results in the 12 lanes in panel A; error bars show standard deviations. *, $P < 0.001$; NS, not significant. (C) Interaction of p65 and AhR mutants. Co-IP of p65 and full-length AhR or mutants expressed in 293T cells, using anti-p65 antibody. AhR FL (full-length) comprises amino acids 1 to 805, AhR ΔC comprises amino acids 1 to 544, and AhR CA comprises amino acids 1 to 276 and 419 to 805; in AhR Y9F, Y9 was mutated to F; and in AhR NLSm 37R, 38H, and 39R were mutated to A, G, and S, respectively. IB, immunoblot; α, anti; +, present.

inflammatory cascade that is dependent on the transcription factor NF-κB (10). Mice with a macrophage-specific conditional deletion of AhR ($AhR^{flox/-}$::LysM Cre) were more susceptible to LPS-induced septic shock than $AhR^{flox/-}$ mice, indicating that the dysfunction of macrophages due to AhR deficiency is one of the major causes of the enhanced susceptibility of AhR KO mice to LPS-induced septic shock (Fig. 2A). Consistent with these observations, isolated AhR KO BMDM secreted much larger amounts of IL-1β and had a slight increase in TNF-α in response to LPS (Fig. 2B). Since IL-1β mRNA levels were not altered between AhR KO and AhR WT BMDM (Fig. 2C), the increased IL-1β secretion is probably not due to the enhanced synthesis but, rather, is likely due to enhanced processing of IL-1β. (16).

We thought that this IL-1β oversecretion by AhR-deficient macrophages might provide clues as to how AhR functions as a physiological immunosuppressor. Microarray analyses to comprehensively investigate the AhR-dependent changes in gene expression that were responsible for increased IL-1β secretion revealed that the levels of expression of Pai-2 and Bcl-2 mRNA were markedly reduced in AhR KO BMDM, which was confirmed by real-time PCR (Fig. 3B). Reconstitution experiments with adenoviruses showed that only Pai-2 expression could significantly suppress IL-1β oversecretion in AhR KO macrophages, while no suppressive effect was observed with Bcl-2 expression (Fig. 3C). It has been reported that there are several pathways for processing IL-1β that lead to its secretion (16). These results indicate that Pai-2 and Bcl-2 are differentially involved in these pathways. Recently, in experiments using ΔIKKβ myeloid mice, Pai-2 has been reported to suppress IL-1β secretion, acting downstream of NF-κB (10). The IL-1β processing that is regulated by the inflammasome involves caspase-1 (16). Consistent with these observations, treatment with caspase inhibitors, Z-YVAD-FMK and Z-VAD-FMK markedly reduced the secretion of IL-1β in AhR KO BMDM (Fig. 3A). It has also been reported that IL-18 processing is regulated by the same mechanism as IL-1β, which is consistent with the marked increase in plasma IL-18 levels ($P < 0.001$) observed in LPS-injected AhR KO mice (Fig. 1B). Stimulation of the inflammasome involving caspase-1 usually requires secondary signals, such as high ATP concentrations. Interestingly, however, the IL-1β oversecretion resulting from AhR deficiency did not seem to require any other stimulation besides LPS, which is in accordance with the report on the IKKβ Δmyeloid mice (10). Further investigation will be required to address the molecular details of Pai-2-regulated IL-1β secretion.

Although it has been reported that Pai-2 mRNA was induced by a typical AhR ligand, TCDD (27), we did not find any obvious XRE sequences (GCGTG) in the 5-kb regions upstream or downstream of the transcription start site of the mouse Pai-2 promoter. However, these promoter regions rendered a reporter gene responsive to LPS (Fig. 5A and E). This sequence search suggested that AhR might not regulate Pai-2 gene expression in the canonical way (i.e., heterodimerized with Arnt) and led us to investigate whether Arnt was involved in LPS-induced Pai-2 regulation. In experiments with Arnt-deficient and Arnt siRNA-expressing macrophages, we demonstrated that AhR enhanced Pai-2 expression in an Arnt-independent manner (Fig. 4D; also see Fig. S1 in the supplemental material). Arnt2 is considered to be another possible alternative (11), but we have previously shown that AhR interacts predominantly with Arnt but not with Arnt2 (27). Therefore, it is highly likely that AhR enhances Pai-2 expression independently of Arnt family proteins (11). It was previously reported that LPS induced Pai-2 expression through activation of NF-κB (21) and that AhR physically interacted with p65 (31) to activate or inhibit gene expression in a context-dependent manner (31). In our reporter gene assay using RAW 264.7 cells, the Pai-2 reporter gene required both NF-κB and AhR for a high level of expression in response to LPS treatment (Fig. 5A). In AhR KO macrophages, LPS treatment induced nuclear translocation of p65 (Fig. 5B), but it was not recruited to the NF-κB-binding site of the Pai-2 gene, which confers LPS inducibility (Fig. 5E), suggesting that AhR is required for recruitment of p65 to this site, which may be a

crossing point between AhR and NF-κB signaling pathways. In WT macrophages, AhR and p65 were recruited to the same DNA sequence by the LPS treatment (Fig. 5E), and they interacted directly (Fig. 5C and 6C), leading to the recruitment of PolII to the TATA sequence of the transcription initiation site. In contrast, p65 was recruited to the Cox-2 promoter in response to LPS treatment in AhR KO macrophages. The detailed molecular basis for how p65 binds differentially to the Pai-2 and Cox-2 genes remains to be investigated.

It was also reported that AhR interacts with RelB on chemokine promoters, such as IL-8, in response to TCDD treatment, enhancing their expression (33). Although an AhR-RelB binding DNA sequence, designated RelBAhRE (GGGTGC AT), was found near the NF-κB site in the Pai-2 promoter, the expression of the Pai-2 (−2.7 kb) Luc reporter gene was not enhanced by RelB and AhR coexpression (data not shown), suggesting that RelB may not function as a partner for AhR in inducing Pai-2 expression. Since the AhR DNA binding activity was suggested by the results of the experiment using the AhR Y9F mutant to be required for AhR-dependent Pai-2 expression (Fig. 6B, bars 3, 4, 9, and 10), the possibility could be raised that an AhR and p65 heterodimer might work as a transcription factor by binding the RelBAhRE sequence. However, the experiments using the reporter gene containing a tandem arrangement of four RelBAhRE sequences did not showed enhanced expression of the reporter gene expression with coexpression of AhR and p65. It remains to be investigated in detail how AhR and p65 activate the Pai-2 promoter. AhR has been reported to have the nuclear localization signal and nuclear export signal sequences and to shuttle between nucleus and cytoplasm. Inhibition of nuclear export of AhR by trichomycin B or phosphorylation reportedly leads to the accumulation of AhR in the nucleus (12). Consistent with these findings, a small part of AhR was observed in the nuclei of macrophages under normal conditions. Upon treatment with LPS, nuclear AhR should accumulate due to phosphorylation downstream of the LPS signaling pathway or p65, reported to be translocated into the nucleus (21), should be recruited to the Pai-2 promoter with the nuclear AhR.

Recently, there have been growing lines of evidence that AhR plays a crucial role in differentiation of the Th cell subsets Th1, Treg, and Th17 from naive CD4 T cells. It was reported that differentiation of these regulatory T cells from AhR KO naive T cells was significantly impaired under their respective polarizing conditions. AhR is reported to be highly induced under these conditions (14, 20, 23, 32), and AhR ligands further stimulated the tendency to their respective differentiations by molecular mechanisms that are largely unknown. In macrophages, AhR was also induced by LPS treatment (Fig. 4A and B) and negatively regulated the secretion of certain inflammatory cytokines, such as IL-1β and IL-18, most likely through the expression of Pai-2. Since AhR is a ligand-activated transcription factor and is known to be ubiquitously expressed in immune cells (13), this raises the possibility that an appropriate AhR ligand may be useful for treating patients with inflammatory disorders.

ACKNOWLEDGMENTS

We thank L. Varesio for kindly providing ANA-1 cells and Y. Watanabe and S. Ooba for mouse maintenance. We also thank Y. Nemoto for clerical work.

This work was funded in part by Solution Oriented Research for Science and Technology from Japan Science and Technology, Japan Science and Technology Agency, Kawaguchi, Japan, and by a grant for Scientific Research from the Ministry of Health, Labor and Welfare, Japan.

REFERENCES

1. **Abbott, B., J. Schmid, J. Pitt, A. Buckalew, C. Wood, G. Held, and J. Diliberto.** 1999. Adverse reproductive outcomes in the transgenic Ah receptor-deficient mouse. Toxicol. Appl. Pharmacol. **155**:62–70.
2. **Baba, T., J. Mimura, N. Nakamura, N. Harada, M. Yamamoto, K. Morohashi, and Y. Fujii-Kuriyama.** 2005. Intrinsic function of the aryl hydrocarbon (dioxin) receptor as a key factor in female reproduction. Mol. Cell. Biol. **25**:10040–10051.
3. **Blasi, E., D. Radzioch, S. Durum, and L. Varesio.** 1987. A murine macrophage cell line, immortalized by v-raf and v-myc oncogenes, exhibits normal macrophage functions. Eur. J. Immunol. **17**:1491–1498.
4. **Bradley, M., L. Zhou, and S. Smale.** 2003. C/EBPbeta regulation in lipopolysaccharide-stimulated macrophages. Mol. Cell. Biol. **23**:4841–4858.
5. **Bruey, J., N. Bruey-Sedano, F. Luciano, D. Zhai, R. Balpai, C. Xu, C. Kress, B. Bailly-Maitre, X. Li, A. Osterman, S. Matsuzawa, A. Terskikh, B. Faustin, and J. Reed.** 2007. Bcl-2 and Bcl-XL regulate proinflammatory caspase-1 activation by interaction with NALP1. Cell **129**:45–56.
6. **Fernandez-Salguero, P., D. Hilbert, S. Rudikoff, J. Ward, and F. Gonzalez.** 1996. Aryl-hydrocarbon receptor-deficient mice are resistant to 2,3,7,8-tetrachlorodibenzo-p-dioxin-induced toxicity. Toxicol. Appl. Pharmacol. **140**:173–179.
7. **Fernandez-Salguero, P., T. Pineau, D. Hilbert, T. McPhail, S. Lee, S. Kimura, D. Nebert, S. Rudikoff, J. Ward, and F. Gonzalez.** 1995. Immune system impairment and hepatic fibrosis in mice lacking the dioxin-binding Ah receptor. Science **268**:722–726.
8. **Fernandez-Salguero, P., J. Ward, J. Sundberg, and F. Gonzalez.** 1997. Lesions of aryl-hydrocarbon receptor-deficient mice. Vet. Pathol. **34**:605–614.
9. **Fujii-Kuriyama, Y., and J. Mimura.** 2005. Molecular mechanisms of AhR functions in the regulation of cytochrome P450 genes. Biochem. Biophys. Res. Commun. **338**:311–317.
10. **Greten, F., M. Arkan, J. Bollrath, L. Hsu, J. Goode, C. Miething, S. Göktuna, M. Neuenhahn, J. Fierer, S. Paxian, N. Van Rooijen, Y. Xu, T. O'Cain, B. Jaffee, D. Busch, J. Duyster, R. Schmid, L. Eckmann, and M. Karin.** 2007. NF-kappaB is a negative regulator of IL-1beta secretion as revealed by genetic and pharmacological inhibition of IKKbeta. Cell **130**:918–931.
11. **Hirose, K., M. Morita, M. Ema, J. Mimura, H. Hamada, H. Fujii, Y. Saijo, O. Gotoh, K. Sogawa, and Y. Fujii-Kuriyama.** 1996. cDNA cloning and tissue-specific expression of a novel basic helix-loop-helix/PAS factor (Arnt2) with close sequence similarity to the aryl hydrocarbon receptor nuclear translocator (Arnt). Mol. Cell. Biol. **16**:1706–1713.
12. **Ikuta, T., Y. Kobayashi, and K. Kawajiri.** 2004. Cell density regulates intracellular localization of aryl hydrocarbon receptor. J. Biol. Chem. **279**:19209–19216.
13. **Kerkvliet, N.** 2009. AHR-mediated immunomodulation: the role of altered gene transcription. Biochem. Pharmacol. **77**:746–760.
14. **Kimura, A., T. Naka, K. Nohara, Y. Fujii-Kuriyama, and T. Kishimoto.** 2008. Aryl hydrocarbon receptor regulates Stat1 activation and participates in the development of Th17 cells. Proc. Natl. Acad. Sci. USA **105**:9721–9726.
15. **Lund, A., M. Goens, B. Nuñez, and M. Walker.** 2006. Characterizing the role of endothelin-1 in the progression of cardiac hypertrophy in aryl hydrocarbon receptor (AhR) null mice. Toxicol. Appl. Pharmacol. **212**:127–135.
16. **Martinon, F., and J. Tschopp.** 2007. Inflammatory caspases and inflammasomes: master switches of inflammation. Cell Death Differ. **14**:10–22.
17. **Mimura, J., K. Yamashita, K. Nakamura, M. Morita, T. Takagi, K. Nakao, M. Ema, K. Sogawa, M. Yasuda, M. Katsuki, and Y. Fujii-Kuriyama.** 1997. Loss of teratogenic response to 2,3,7,8-tetrachlorodibenzo-p-dioxin (TCDD) in mice lacking the Ah (dioxin) receptor. Genes Cells **2**:645–654.
18. **Minsavage, G. D., S. Park, and T. A. Gasiewicz.** 2004. The aryl hydrocarbon receptor (AhR) tyrosine 9, a residue that is essential for AhR DNA binding activity, is not a phosphoresidue but augments AhR phosphorylation. J. Biol. Chem. **279**:20582–20593.
19. **Muruve, D., V. Pétrilli, A. Zaiss, L. White, S. Clark, P. Ross, R. Parks, and J. Tschopp.** 2008. The inflammasome recognizes cytosolic microbial and host DNA and triggers an innate immune response. Nature **452**:103–107.
20. **Negishi, T., Y. Kato, O. Ooneda, J. Mimura, T. Takada, H. Mochizuki, M. Yamamoto, Y. Fujii-Kuriyama, and S. Furusako.** 2005. Effects of aryl hydrocarbon receptor signaling on the modulation of TH1/TH2 balance. J. Immunol. **175**:7348–7356.
21. **Park, J., F. Greten, A. Wong, R. Westrick, J. Arthur, K. Otsu, A. Hoffmann, M. Montminy, and M. Karin.** 2005. Signaling pathways and genes that inhibit pathogen-induced macrophage apoptosis—CREB and NF-kappaB as key regulators. Immunity **23**:319–329.
22. **Petrulis, J., and G. Perdew.** 2002. The role of chaperone proteins in the aryl hydrocarbon receptor core complex. Chem. Biol. Interact. **141**:25–40.

23. **Quintana, F., A. Basso, A. Iglesias, T. Korn, M. Farez, E. Bettelli, M. Caccamo, M. Oukka, and H. Weiner.** 2008. Control of T(reg) and T(H)17 cell differentiation by the aryl hydrocarbon receptor. Nature **453**:65–71.
24. **Schmidt, J., G. Su, J. Reddy, M. Simon, and C. Bradfield.** 1996. Characterization of a murine Ahr null allele: involvement of the Ah receptor in hepatic growth and development. Proc. Natl. Acad. Sci. USA **93**:6731–6736.
25. **Schreiber, E., P. Matthias, M. Müller, and W. Schaffner.** 1989. Rapid detection of octamer binding proteins with 'mini-extracts,' prepared from a small number of cells. Nucleic Acids Res. **17**:6419.
26. **Schwartz, B., and J. Bradshaw.** 1992. Regulation of plasminogen activator inhibitor mRNA levels in lipopolysaccharide-stimulated human monocytes. Correlation with production of the protein. J. Biol. Chem. **267**:7089–7094.
27. **Sekine, H., J. Mimura, M. Yamamoto, and Y. Fujii-Kuriyama.** 2006. Unique and overlapping transcriptional roles of arylhydrocarbon receptor nuclear translocator (Arnt) and Arnt2 in xenobiotic and hypoxic responses. J. Biol. Chem. **281**:37507–37516.
28. **Sogawa, K., R. Nakano, A. Kobayashi, Y. Kikuchi, N. Ohe, N. Matsushita, and Y. Fujii-Kuriyama.** 1995. Possible function of Ah receptor nuclear translocator (Arnt) homodimer in transcriptional regulation. Proc. Natl. Acad. Sci. USA **92**:1936–1940.
29. Reference deleted.
30. **Takagi, S., H. Tojo, S. Tomita, S. Sano, S. Itami, M. Hara, S. Inoue, K. Horie, G. Kondoh, K. Hosokawa, F. Gonzalez, and J. Takeda.** 2003. Alteration of the 4-sphingenine scaffolds of ceramides in keratinocyte-specific Arnt-deficient mice affects skin barrier function. J. Clin. Investig. **112**:1372–1382.
31. **Tian, Y., S. Ke, M. Denison, A. Rabson, and M. Gallo.** 1999. Ah receptor and NF-kappaB interactions, a potential mechanism for dioxin toxicity. J. Biol. Chem. **274**:510–515.
32. **Veldhoen, M., K. Hirota, A. Westendorf, J. Buer, L. Dumoutier, J. Renauld, and B. Stockinger.** 2008. The aryl hydrocarbon receptor links TH17-cell-mediated autoimmunity to environmental toxins. Nature **453**:106–109.
33. **Vogel, C., E. Sciullo, W. Li, P. Wong, G. Lazennec, and F. Matsumura.** 2007. RelB, a new partner of aryl hydrocarbon receptor-mediated transcription. Mol. Endocrinol. **21**:2941–2955.

Journal of Andrology, Vol. 30, No. 6, November/December 2009

Identification of Rat Prostatic Secreted Proteins Using Mass Spectrometric Analysis and Androgen-Dependent mRNA Expression

NARIAKI FUJIMOTO,* TOMOHARU SUZUKI,† SHIGERU OHTA,† AND SHIGEYUKI KITAMURA‡

*From the *Department of Developmental Biology, Research Institute for Radiation Biology and Medicine (RIRBM), Hiroshima University, Hiroshima, Japan; the †Department of Xenobiotic Metabolism and Molecular Toxicology, Institute of Pharmaceutical Sciences, Hiroshima University School of Medicine, Hiroshima, Japan; and the ‡Department of Health Pharmaceutical Sciences, School of Pharmacy, Nihon Pharmaceutical University, Saitama, Japan.*

ABSTRACT: Rats have been used to study the function and development of the mammalian prostate. Identification of prostatic secreted proteins is important in order to better understand their physiological function. Previous investigations have showed that prostatein, cysteine-related protein 1, and kallikrein S3 are in the ventral prostate (VP), whereas the proteins probasin, prostate secretory peptide 94, transglutaminase 4, and carbonic anhydrase II are produced in the lateral prostate, dorsal prostate (DP), and anterior prostate. They are also useful markers when looking at androgen dependency as well as prostate-specific expression. Although some of the rat prostatic proteins have been investigated well, the overall protein expression profile of the prostate has not been examined. In the present study, the secretions from the rat prostate were subjected to 2-dimensional gel electrophoresis followed by mass spectrometric analysis. In addition to the previously known proteins, proteome analysis revealed several new secreted proteins, including spermine-binding protein and a protein similar to immunoglobulin-binding protein. In addition, epididymal secreted protein 1 and peroxiredoxin 6 were found in the DP, while glucose-regulated protein 78 was identified in all lobes of the prostate. Castration of the animals led to a decrease in the mRNAs of all of these secreted proteins. While the mRNAs of prostatic proteins became almost completely absent in the VP, the reductions in the other lobes were limited. A novel view of rat prostate secretion from our results should contribute to an understanding of the biological functions of the prostate gland.

Key words: Rat prostate, secretion, proteome analysis, lobe-specific, androgen regulation.

J Androl 2009;30:669–678

In order to study prostate morphology, development, and pathology, as well as androgen-regulated gene expression, rat models have been widely used (Cunha et al, 1987). The rodent prostate consists of the ventral prostate (VP), lateral prostate (LP), dorsal prostate (DP), and anterior prostate (AP, or coagulating gland). The main physiological function of the prostate gland is to produce and secrete prostatic proteins. These proteins have been studied in rats as well as humans, especially to understand the androgen-dependent regulation of expression and to identify possible markers of prostate cancer (Spence et al, 1989; Donjacour et al, 1990; Heyns, 1990; MacDonald et al, 1996; Vercaeren et al, 1996; Imasato et al, 2001). The major human prostatic secreted proteins are prostate-specific antigen (PSA), prostate secretory peptide 94 (PSP94), and prostatic acid phosphatase (PAP) (Lee et al, 1986). In rats, the composition of prostatic proteins has been shown to be very different, because it is believed that only PSP94 is in common with humans, and the production of each protein varies among the lobes (Fernlund et al, 1996; Xuan et al, 1999). Recently we identified major prostatic secretory proteins in mice (Fujimoto et al, 2006) and found that they were not similar to previously known rat prostatic secretions. Considering the morphological and functional similarities of the prostate gland in 2 species, these discrepancies were puzzling. In the present study, then, the secretions from rat prostatic lobes were subjected to 2-dimensional gel electrophoresis, followed by matrix-assisted laser desorption ionization–time of flight mass spectrometric analysis, to determine the major prostatic secretory proteins in rats with a view to comparing their profiles with those in mice and humans. Additionally, a

Supported in part by a Grant-in-Aid (H19-kagaku-Ippan-003) from the Ministry of Health, Labor and Welfare, Japan and a Grant-in-Aid (17510046) from the Ministry of Education, Culture, Sports, Science and Technology, Japan.

Correspondence to: Dr Nariaki Fujimoto, Department of Developmental Biology, Research Institute for Radiation Biology and Medicine, Hiroshima University, 1-2-3 Kasumi, Minami-ku, Hiroshima 734-8553, Japan (e-mail: nfjm@hiroshima-u.ac.jp).

Received for publication March 27, 2008; accepted for publication June 1, 2009.

DOI: 10.2164/jandrol.108.005553

quantitative reverse transcription–polymerase chain reaction (RT-PCR) method was employed to examine the androgen dependence of the transcriptional regulation of the secretory proteins.

Materials and Methods

Animals

Animal experiments were approved by the Animal Experiment Committee of Hiroshima University (document B05-4) and conducted in accordance with "A Guide for the Care and Use of Laboratory Animals of Hiroshima University." Male F344 rats were purchased from Charles River Japan Co (Kanagawa, Japan) and maintained with free access to a basal diet and tap water. For proteome analysis, three 11-week-old rats were killed under ether anesthesia and their prostates were carefully resected. Each of the prostate lobes was dissected under a microscope. For RNA isolation, the lobes were immediately fixed in RNA Later solution (Ambion Inc, Austin, Texas). For the castration and hormone replacement study, the animals were divided into 5 groups: castrated, castrated and testosterone-injected (1, 4, and 24 hours), and intact, with 5 animals per group. Surgical castration was performed when the animals reached 11 weeks of age, and the animals were then allowed to recover for 1 week. Testosterone propionate (Wako Junyaku KK, Osaka, Japan) was dissolved in vehicle oil, Panacete 810 (Nippon Oils and Fats Co, Ltd, Tokyo, Japan), and the solution was administered IP at 5 mg/kg body weight. The animals were sacrificed under ether anesthesia 1, 4, and 24 hours after testosterone injection, and the prostate lobes were collected for RNA extraction.

Preparation of Secretion Samples

The preparation of secretion samples was performed based on a previously reported method (Donjacour et al, 1990). Each dissected prostate lobe from a 12-week-old rat was rinsed well in saline and placed on a 35-mm culture dish with 100 μL of saline containing a 1% protease inhibitor mixture (P8340; Sigma, St Louis, Missouri). Each lobe was cut into 4 or 5 pieces, left to stand for 5 minutes, and transferred to a 1.5-mL microcentrifuge tube. After centrifugation at 10 000 × *g* for 5 minutes at room temperature, the supernatant was collected as the secretion sample. The incubation time of 5 minutes was chosen because inner cellular contamination (glyceraldehyde-3-phosphate dehydrogenase) was confirmed to be low by 5 minutes (Fujimoto et al, 2006). The protein concentration of each sample solution was determined with a Protein Assay kit (Bio-Rad Laboratories Inc, Hercules, California). Because prostatic proteins are known to be glycosylated, the samples were digested with Peptide N-Glycosidase (PNGase) F, which removes all types of N-linked glycosylation, to improve the mass spectrometric identification of proteins. Prior to electrophoresis, each of the samples was incubated with PNGase F (50 U/μg protein; New England Biolabs, Ipswich, Massachusetts) at 37°C for 1.5 hours for deglycosidation.

Two-Dimensional Polyacrylamide Gel Electrophoresis

First-dimensional isoelectric focusing with immobilized pH gradients was performed using Immobiline DryStrip (GE Healthcare Life Sciences Co, Piscataway, New Jersey) and the Ettan IPGphor system (GE Healthcare) according to the manufacturer's protocol. For analytical 2-dimensional polyacrylamide gel electrophoresis (2D-PAGE), 10 μg of deglycosidated protein was applied to a 7-cm Immobiline DryStrip (pI = 3–11, nonlinear gradient). After rehydration, the strip was isoelectrofocused (15 kVh). The Immobiline gel was then treated with a sodium dodecyl sulfate (SDS) equilibration buffer (50 mM Tris HCl, pH 8.8, 6 M urea, 30% glycerol, and 2% SDS) containing 10 mg/mL dithiothreitol for 15 minutes, followed by the same buffer containing 25 mg/mL iodoacetamide. The Immobiline gel was then placed on the second SDS–polyacrylamide gel electrophoresis (SDS-PAGE) slab gel with 5%–20% gradient (SuperSep precast gel, Wako Jyunyaku) and overlaid with hot agarose solution to connect the 2 gels. The second electrophoresis was run at a constant current of 20 mA. The gel was fixed with 50% methanol and 7% acetic acid, stained overnight in Sypro Ruby (Invitrogen Corp, Carlsbad, California), and destained with 10% methanol and 7% acetic acid. The stained gels were scanned with a Molecular Imager FX Pro (Bio-Rad), with excitation at 532 nm. In the case of preparative 2D-PAGE for mass spectrometric analysis, 60 μg of total protein was subjected to electrophoresis as described above and then stained with silver nitrate by incubation with 0.2 g/L $Na_2S_2O_3$ for 1 minute followed by 1 g/L $AgNO_3$ for 20 minutes on ice, and washed with 20 g/L Na_2CO_3 containing 0.1% HCHO.

Mass Spectrometry

Protein spots were excised from the polyacrylamide gel and the silver nitrate was removed with 15 mM $K_3[Fe(CN)_6]$ and 50 mM $Na_2S_2O_3$. The gel pieces were incubated in distilled water several times for 1-hour periods, then incubated with CH_3CN for 10 minutes, and dried in a centrifuge-vacuum concentration system. Each gel piece was incubated with a 20-μL aliquot of 10 μg/mL trypsin solution (sequence grade, Sigma) for 30 minutes on ice. Excess trypsin solution was removed, and the gel piece was incubated overnight at 35°C. To extract the digested peptides, 10 μL of a 70% CH_3CN solution containing 0.1% trifluoroacetic acid was added to each gel piece. A 0.5-μL aliquot of the extract solution was spotted onto a target plate for an UltraFlex mass spectrometer (Bruker Daltonics, Bremen, Germany) along with 0.5 μL of 10 mg/mL α-cyano-4-hydroxycinnamic acid (mass spectrometry [MS] grade; Nacalai Tesque Co, Kyoto, Japan). MS was performed using an accelerating voltage of 20 kV, with data acquisition between 1000 and 4000 daltons. Some of the fragment peaks were further analyzed by MS/MS. The MS and MS/MS data were evaluated with Biotools software (Bruker Daltonics) in combination with a peptide mass fingerprinting analysis system, MASCOT Ver. 2.1 (Matrix Science, London, United Kingdom). The peptide mass fingerprinting was performed with reference to the MSDB and NCBInr databases, with the terminal modifications of the peptides set as fixed carbamidomethyl and flexible oxidation ends. The peptide mass tolerance was set to 0.3%.

Table 1. *Quantitative PCR primers for rat genes*

Gene	GenBank Accession No.	5′ Primer (5′→3′)	3′ Primer (5′→3′)
Prostatein C3	M71245	5′-CAGTGGTTCTGGCTGCAGTATT	5′-CTAGAAAACACTGCTTGAATTGCTTC
Cysteine-rich protein 1	S57980	5′-TGCTCCTACTGGCCATCTTTG	5′-TGTCAGCACTGTGCGTGTTG
Kallikrein S3	M11566	5′-AATTCCCAACCCTGGCAAGT	5′-CGCTGAGCAAAGGGTTCATC
Spermine-binding protein	NM_013024	5′-TACGGATCCCGGTCACTAAAA	5′-AACACCAAAGGTGACCACTCG
Transglutaminase 4	RATTRNGLT	5′-GGCAAGAACATCAGCACCAA	5′-TGTCCGAGAGTTGAGCTTGTCA
IgG-binding protein–like protein	BC099756	5′-CAGAGGAGTCAGTTCTCATTGAAAAC	5′-TTGCATGGGTCTTTGTTGATG
Carbonic anhydrase II	NM_019291	5′-GCTCAAGGAACCCATTACTGTCA	5′-TTTAAAGGACGCCTTGATCTTTCT
Epididymal secretory protein 1	NM_173118	5′-TACTAGCGGCACTCAGTCCCA	5′-CCGGCAGCTTATTCAGGTAGC
78-kDa glucose-regulated protein	NM_013083	5′-ACTGGAATCCCTCCTGCTCC	5′-GTTTTGGTCATTGGTGATGGTG
Peroxiredoxin 6	NM_053576	5′-AGCCTTAAGTCTGCGGGAACT	5′-GCCATTTCCATTTAATGAGCCA
Probasin	NM_019125	5′-CCTCCTGCTCACACTGGATGT	5′-GCGACGGAAGTAGGTCCTCA
PSP94	U65486	5′-GATCACCTGCTGCACCAAAAC	5′-TTCCTGGGTTCGTCCGTTC
β-actin	X03765	5′-CTGTCCCTGTATGCCTCTGGTC	5′-TGAGGTAGTCCGTCAGGTCCC

Abbreviation: PSP94, prostate secretory peptide 94.

Quantification of mRNAs by Real-Time RT-PCR

Total RNA was prepared from each lobe of the prostate using an RNA isolation kit, NucleoSpin RNA II (Machery-Nagel GmbH & Co KG, Düren, Germany), and 2 μg of the total RNA was reverse transcribed as described previously (Fujimoto et al, 2004). An ABI Prism 7700 (PerkinElmer Life Sciences, Boston, Massachusetts) was employed for quantitative measurement of the cDNA using a QuantiTect Sybr Green PCR kit (Qiagen, Valencia, California). Specific primer sets with a melting temperature of about 59°C were designed for each mRNA (Table 1). Prior to quantitative analysis, PCR products were prepared separately and purified by gel electrophoresis. The DNA sequences were confirmed with a capillary DNA sequencer, ABI 310 (PerkinElmer Life Sciences). The extracted fragments were used as standards for quantification. The PCR conditions were 15 minutes of initial activation followed by 45 cycles of 20 seconds at 94°C, 30 seconds at 58°C, and 40 seconds at 72°C. All mRNA contents were normalized with reference to β-actin mRNA.

Statistical Analysis

Statistical comparisons were made using Student's *t* test.

Results

2D-PAGE and Identified Proteins

Secretory proteins from all of the lobes were treated with PNGase F and subjected to 2D-PAGE analysis. Because of the limitation of the pore size of the immobilized pH gradient gel for isoelectric focusing, proteins with a molecular weight over 100 kDa could not be analyzed in the 2D-PAGE. The gels were stained and the major spots were selected for MS analysis (Figure 1). Two sets of prostate secretions from independent control mice were analyzed and provided identical patterns. The spots were successfully identified, and the results are summarized in Table 2. Prostatein, cystatin-related protein 1 (CRP1), and kallikrein S3 (KS3) were major proteins, along with spermine-binding protein (SBP) in the VP. Similar proteins were found in the LP, with the exception of the additional secretion of carbonic anhydrase II (CA2). In the DP, a100-kDa protein, which showed a thin spot because of the pore size limitation of the Immobiline gel, was identified as a predicted protein similar to immunoglobulin-binding protein. Transglutaminase 4 (TGase4), CA2, epididymis-specific protein 1 (ESP1), and peroxiredoxin 6 (PRdx6) were also found. Similar secreted proteins were found in the AP. Contamination by the serum proteins, including albumin, transferrin, and aldose reductase, was unavoidable especially in the DP sample.

Lobe-Specific mRNA Expression of Identified Secreted Proteins

The expression of the identified proteins in the prostate was further confirmed by examining their mRNA levels; the results are summarized in Table 3. The lobe-specific expression of secreted proteins was evident. Prostatein C3, CRP1, and KS3 mRNAs were abundant in the VP and LP. The mRNA expression of SBP was also VP/LP specific. High-level expression of immunoglobulin G–binding protein-like protein (IgGBPLP) and TGase4 mRNA was detected only in the DP and AP. Probasin and PSP94 mRNAs, proteins that were not identified in 2D gel electrophoresis, were specific to the LP/DP. ESP1 and PRdx6 were specific to the DP.

Androgen Dependency of mRNA Expression of Identified Secreted Proteins

The transcriptional regulation of the identified proteins by androgen was examined by comparing mRNA levels

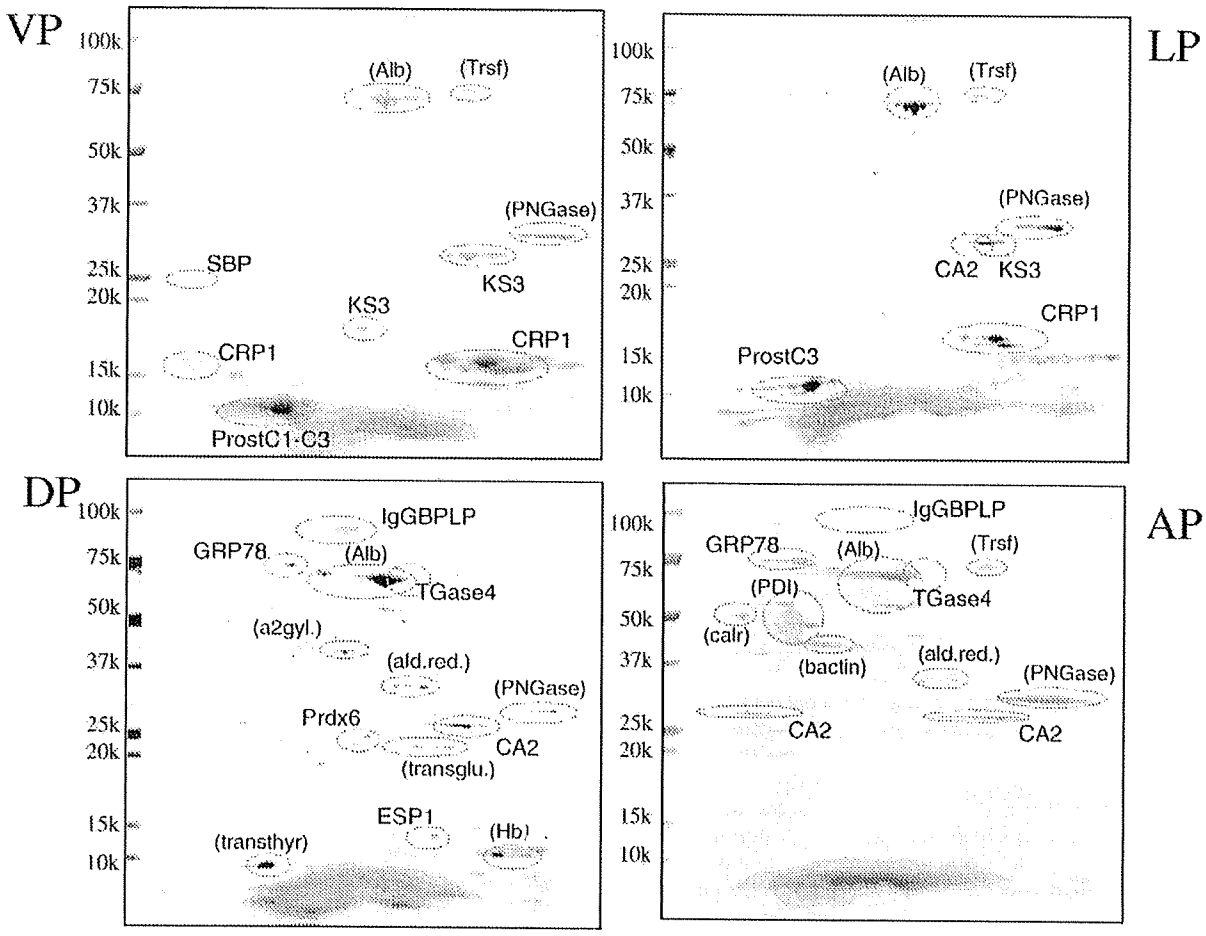

Figure 1. Two-dimensional polyacrylamide gel electrophoresis (2D-PAGE) analysis of rat prostate secretory proteins. Each sample from the ventral prostate (VP), lateral prostate (LP), dorsal prostate (DP), and anterior prostate (AP) was treated with Peptide N-Glycosidase (PNGase) F and applied to an immobilized pH gradient gel, followed by a second sodium dodecyl sulfate polyacrylamide gel electrophoresis (SDS-PAGE). The gels were stained with Sypro Ruby. The identified spots are indicated in the figure. Serum albumin (Alb), transferrin (Trsf), and hemoglobin (Hb) were considered to be due to serum contamination.

among the castrated, castrated and testosterone-treated, and intact animals (Figure 2). The mRNA levels were normalized by the β-actin levels, which were not affected by castration or testosterone treatment. The mRNA levels of the identified secreted proteins decreased 1 week after castration, although the extent of the decrease differed among the proteins. Prostatic protein mRNAs in the VP fell to an almost undetectable level after castration, but the probasin in the LP, for instance, fell to only one-third its original level. The mRNA levels increased after a single injection of testosterone, but in different manners. IgGBPLP and PRdx6 mRNAs increased significantly in 1 hour after an injection, whereas the others started to increase afterward. The manner of androgen response is varied among different lobes (Figure 3). In case of CA2, the mRNA was significantly regulated by androgen in the LP, but unchanged in the DP. TGase4 and IgGBPLP mRNAs reached to above the intact control level in the AP but not in the DP.

Discussion

In the present study, the major secretory proteins of the rat prostate were identified by mass spectrometric analysis after 2D gel electrophoresis. In addition to previously known prostatic proteins, including prostatein, CRP1, and KS3 in the VP as well as TGase4 and CA2 in the LP/DP/AP, SBP, IgGBPLP, ESP1, 78-kDa glucose-regulated protein (GRP78), and PRdx6 were found in the prostatic secretions. The mRNAs for these proteins were expressed in a lobe-specific manner and

Table 2. *Identified rat prostatic secretory proteins*[a]

Abbreviation	Protein Name	Accession No.	Observed MW/pI	Theoretical MW/pI	P	Sequence Coverage (%)
PrstC3	prostatein C3	P02780	11/4~5	11/5.5	1.00	34
CRP1	cysteine-rich protein 1	AAA42345	17/8~9	19/9.6	1.00	49
KS3	kallikrein S3	AAH61771	30/7	29/7.8	1.00	40
SBP	spermine-binding protein	NP_037156	25/4	31/3.7	1.00	27
TGase	transglutaminase	NP_073204	75/8	76/7.9	1.00	55
IgBPLP	IgG-binding protein-like protein	AAH99756	100/5~6	216/5.6	1.00	17
CA2	carbonic anhydrase II	NP_062164	30/7~8	29/7.0	1.00	58
ESP1	epididymal secretory protein 1	NP_775141	15/7	17/8.9	1.00	42
GRP78	78-kDa glucose-regulated protein	AAA41277	75/5	71/5.5	1.00	49
PRdx6	peroxiredoxin 6	NP_446028	30/7~8	29/7.1	1.00	29

Abbreviations: MW, molecular weight; pI, isoelectric point.
[a] Neither probasin (NP_061998) nor PSP94 (NP_062061) was identified in the 2D gel.

were found to be regulated by androgen. Identifying several new prostatic proteins in rats, our present study put forth a novel view of rat prostatic secretions and reveals some similarities in prostatic secretions of rats and mice.

The identification and characterization of prostatic secretory proteins has drawn interest because these proteins may be good candidates for prostate cancer makers and as gene expression models of androgen-dependent regulation (Spence et al, 1989; Donjacour et al, 1990; Heyns 1990; MacDonald et al, 1996; Vercaeren et al, 1996; Imasato et al, 2001). The major human prostatic secreted proteins are PSA, PSP94, and PAP (Lee et al, 1986). The rodent prostate is morphologically very different from that of the human, and it is believed that PSP94 is the only secretory protein common to both species (Fernlund et al, 1996; Xuan et al, 1999). In addition, previous studies have suggested large differences even between rat and mouse in prostatic secretions, in spite of the morphological similarities (Donjacour et al, 1990). However, there had been very few reports about mouse prostatic secretions; thus, we recently performed an investigation identifying mouse secretions (Fujimoto et al, 2006). Our study showed that the mouse VP secretions are composed of SBP, serine protease inhibitor KT3, PRdx6, GRP78, and "91-kDa protein," whereas the LP/DP and AP secrete IgGBPLP, experimental autoimmune prostatitis antigen protein 2, PRdx6, GRP78, zinc-α2- glycoprotein, and phospholipase Cα. The present data show that SBP, IgGBPLP, PRdx6, GRP78, and PSP94 are all common to the prostatic secretions of rats and mice.

The secretion of the rat VP was reported to contain prostatein (about 50% of the secretion), CRP1 (10%), and kallikreins (Vercaeren et al, 1998). Prostatein consists of components, C1 + C3 and C2 + C3, linked by disulfide bridges (Heyns 1990). The 22-kDa CRP1 was named after its sequence homology with cystatins, a group of cysteine protease inhibitors (Vercaeren et al, 1996). KS3, one of the tissue kallikreins (serine proteases), is also abundantly expressed in the VP (Clements et al, 1988). SBP is one of the major secretions of the mouse VP and is reported to be under the control of androgen (Mills et al, 1987). Our results indicate that SBP is also secreted and hormonally regulated in the rat VP.

Among the secretions of the LP/DP/AP, probasin (originally named after prostatic basic protein) is structurally related to the lipocalin superfamily, which suggests that this protein is a ligand-carrier protein, although its ligands and function are not presently known (Spence et al, 1989). Its mRNA was expressed greatly in the LP/DP, but it was not found by mass spectrometric analysis in the present study. This may suggest that probasin is mainly localized intracellularly in the nuclei rather than in the secretions. An early study reported that this protein was localized in the lumen and acinal regions of the epithelium (Dodd et al, 1983). Similarly, PSP94 was not identified as a protein spot in our 2D gels, whereas a substantial amount of mRNA was detected. PSP94, also known as β-microseminoprotein, is a nonglycosylated and cysteine-rich protein with 94 amino acids (Fernlund et al, 1996). It was first isolated from human seminal plasma and found to be one of the major prostatic proteins in humans. It is expressed in rat LP/DP (Kwong et al, 2000), as confirmed in the present study, although it is found in both the VP and LP/DP in the case of the mouse. The function of this protein may be immunoglobulin binding to suppress the activation of B cells in the female reproductive tract. This protein may also function as a suppressor of tumor growth and metastasis (Beke et al, 2007). Another "prostatic protein" not found in the 2D gel was seminal vesicle secretion II, whose mRNA was abundantly expressed in the LP in our previous study and others (Kwong et al, 2000; Suzuki et al, 2007).

Table 3. *mRNA levels of identified proteins in each prostatic lobe in 12-week-old rats*[a]

	PrstC3	CRP1	KS3	SBP	TGase4	IgBPLP	CA2	ESP1	GRP78	PRdx6	Prob	PSP94
VP	233.0 ± 15.0	63.0 ± 5.3	12.1 ± 0.9	3.4 ± 0.1	0	0	0	0	1.5 ± 0.1	0	1.7 ± 0.5	0
LP	52.0 ± 3.4	14.6 ± 1.0	2.9 ± 1.0	1.2 ± 0.1	3.0 ± 1.3	0	8.4 ± 2.0	0	1.2 ± 0.2	0	44.1 ± 16.3	14.5 ± 5.4
DP	7.7 ± 4.6	0.8 ± 0.5	0	0	79.3 ± 2.2	55.7 ± 7.1	7.2 ± 0.7	1.3 ± 0.1	1.8 ± 0.1	1.4 ± 0.3	18.8 ± 2.6	12.3 ± 1.5
AP	2.8 ± 1.1	0.7 ± 0.3	0	0	27.0 ± 7.0	33.4 ± 7.9	2.1 ± 0.2	0	0.8 ± 0.4	0	2.4 ± 0.2	1.2 ± 0.4

Abbreviations: AP, anterior prostate; CA2, carbonic anhydrase II; CRP1, cystatin-related protein 1; DP, dorsal prostate; ESP1, epididymis specific protein 1; GRP78, 78-kDa glucose-regulated protein; IgGBPLP, immunoglobulin G–binding protein-like protein; KS3, kallikrein S3; LP, lateral prostate; PRdx6, preroxiredoxin 6; Prob, probasin; PrstC3, prostatein C3; PSP94, prostate secretory peptide 94; SBP, spermine binding protein; TGase4, transglutaminase 4; VP, ventral prostate.

[a] Mean ± SEM (n = 5). Values are mRNA levels divided by β-actin mRNA levels (mol/mol β-actin). Twelve-week-old male F344 rats were sacrificed. Total RNA was isolated from each prostate lobe and mRNA levels were measured by real-time reverse transcriptase–polymerase chain reaction.

The major secretions in the DP/AP were IgGBPLP and TGase4. IgGBPLP is the predicted protein (AAH99756) derived from the cDNA sequence RGD1311906, which was calculated to contain 1914 amino acids, with a molecular weight of 206 kDa. Because peptide sequencing by the peptide-mass fingerprinting method covered several parts of the entire predicted sequence (17% coverage), the 100-kDa spot probably contains a mixture of cleaved fragments derived from the 206-kDa protein, although this remains to be confirmed. This IgGBPLP seems to be identical to the immunoglobulin G (IgG)-binding protein of 115 kDa reported by Wilhelm et al (2002), who also demonstrated that this protein was actually capable of binding IgG. The role of IgGBPLP may thus be to reduce the immunological responses in the female reproductive tract via IgG binding. TGase4 is a prostate-specific isozyme of transglutaminases (Ca2+-dependent intracellular and extracellular enzymes). TGase4 catalyzes the cross-linking between proteins and/or polyamines, and was first discovered as Factor XIII (Seitz et al, 1990; Ho et al, 1992). In the rat prostate, it had been previously known as dorsal prostatic secretory protein-1 (Wilson and French 1980) and was then identified as a member of the transglutaminase gene family (Ho et al, 1992). In rodents, TGase4 plays a role in producing a stable coagulum by catalyzing the isopeptide cross-link. It is also found expressed in the human prostate. CA2 has been known to be expressed at a very high level in prostate tissue (Fischer and Mawson, 1952) and to be expressed in the epididymal duct epithelium as well. This protein is secreted via the apocrine mode (Wilhelm, 1998). The physiological function of CA2 is linked to the secretion of bicarbonate and proton ions into the seminal fluid (Harkonen et al, 1991).

PRdx6 is a new component of the rat prostatic secretion found in the present study. Because it is an antioxidant enzyme that reduces peroxide and alkyl hydroperoxide to water and alcohol, respectively (Wang et al, 1997), it would presumably act as a seminal plasma antioxidant. GRP78 belongs to the heat shock protein 70 family, which were previously considered to be intercellular proteins. However, a recent proteomic analysis of human prostasomes revealed the presence of heat shock proteins in prostatic secretions (Girotti et al, 1992). In addition, heat shock protein 70 has been reported to be secreted from a variety of prostatic cell lines and to show growth-inhibitory activity (Jones et al, 2004; Wang et al, 2004). GRP78 may have similar activity in the rat prostate. ESP1 is a protein identified as a major epididymis secretory protein. It belongs to the lipocalin superfamily and may be related to cholesterol transport (Girotti et al, 1992). Interestingly,

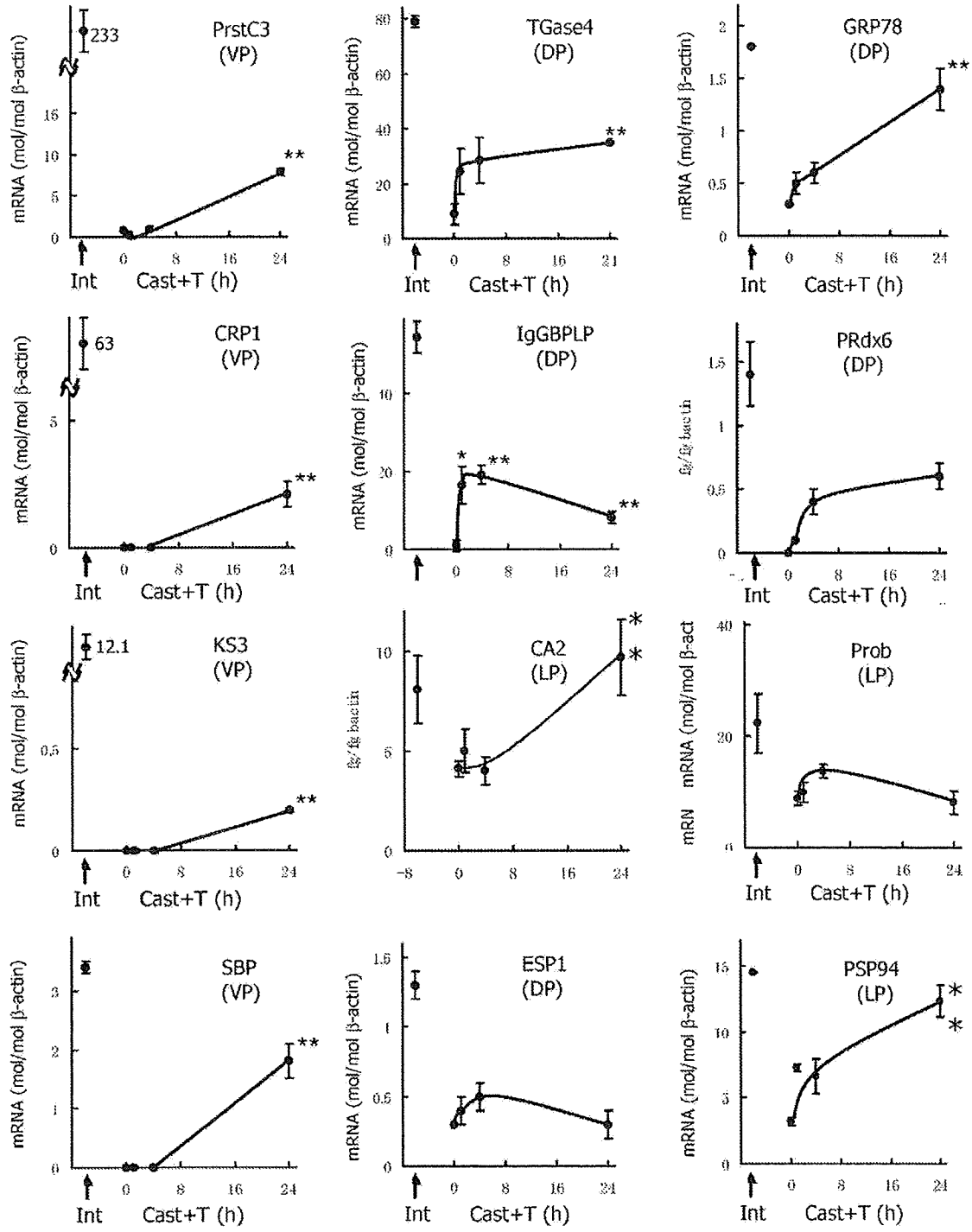

Figure 2. The mRNA levels of the prostatic proteins in the designated prostatic lobes at 0, 1, 4, and 24 hours after a testosterone (T) injection (5 mg/kg body weight, IP) in rats castrated a week previously. Bar indicates mean ± SEM. n = 5. * indicates $P < .05$ vs 0 hours; ** $P < .01$ vs 0 hours.

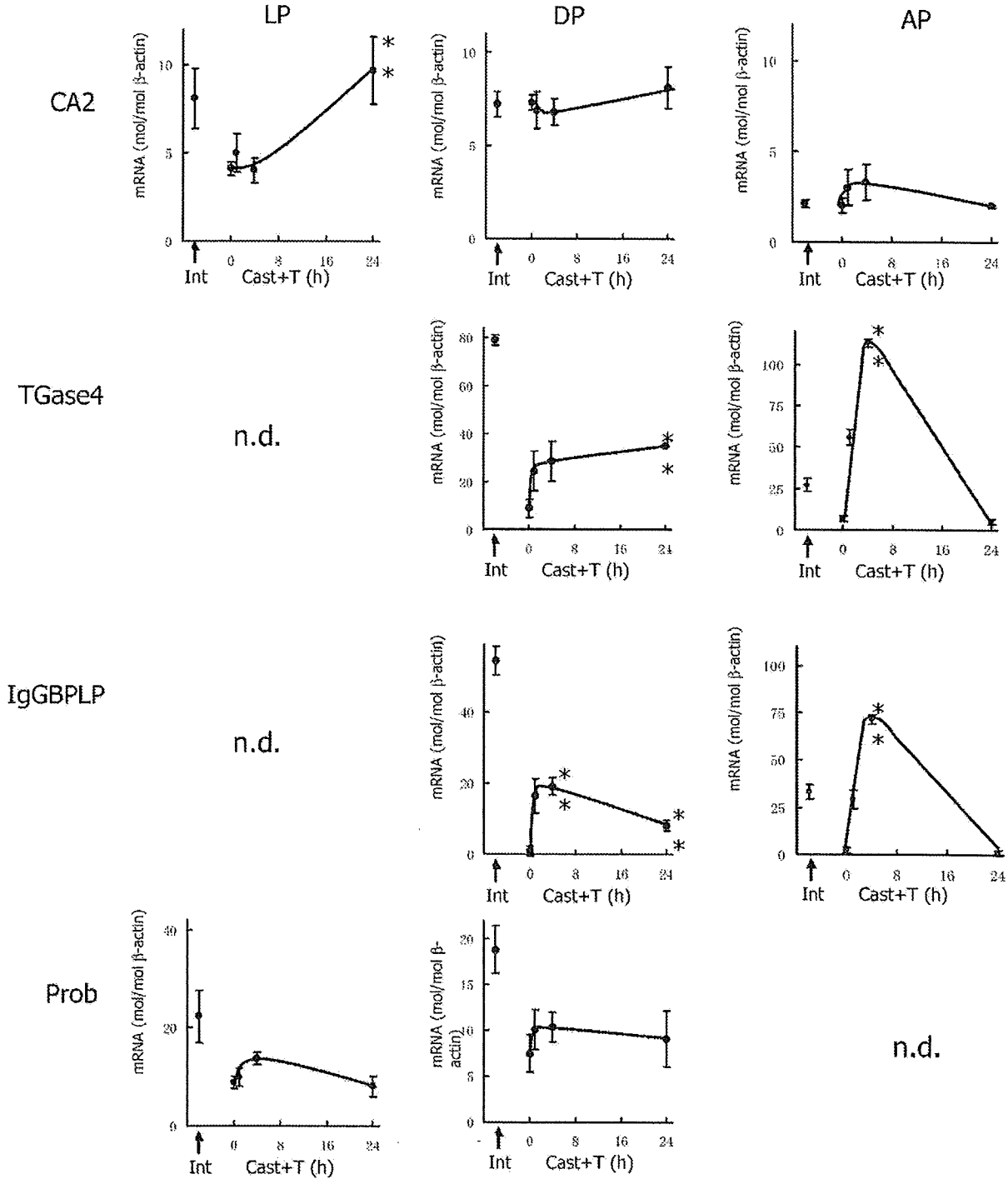

Figure 3. The mRNA levels of the prostatic proteins in the lateral prostate (LP), dorsal prostate (DP), and anterior prostate (AP) at 0, 1, 4, and 24 hours after a testosterone (T) injection (5 mg/kg body weight, IP) in rats castrated a week previously. Bar indicates mean ± SEM. n = 5. ** indicates $P < .05$ vs 0 hours; **$P < .01$ vs 0 hours; n.d., not detected.

ESP1 turned out to be a gene that causes Niemann-Pick type C disease, a fatal neurodegenerative disorder characterized by a lysosomal accumulation of cholesterol and other lipids within the cells of patients (Naureckiene et al, 2000).

Prostatic proteins are generally regulated by androgen, although the responses differ greatly depending on the proteins and prostatic lobes that are expressed. In a previous study, we demonstrated stricter androgen responses in the VP as compared to the other lobes. For instance, castration decreased probasin mRNA expression to 2% of the control level after a week, while the decrease in the DP was only to 40% (Suzuki et al, 2007), although the genomic upstream regions contain consensus androgen-responsive elements (AREs) that were functional promoters in in vitro reporter assay (Rennie et al, 1993). We examined the androgen-dependent transcriptional regulation of the identified prostate proteins after a single injection of testosterone in castrated animals. The serum testosterone level well exceeded the control level within 1 hour and was still high 24 hours after the injection, as we previously reported (Suzuki et al, 2007). Within 24 hours, most of the mRNA levels had significantly increased, which clearly demonstrated the androgen inducibility of their mRNA levels. In the present study, we found that newly identified IgGBPLP and TGase4 mRNAs were rather strictly regulated by androgen in the DP and the AP. They provide useful models for androgen responsive gene transcription in the DP/AP. The genomic upstream regions of these genes, however, do not contain ARE or ARE-like motifs (Q49907_rat gene in chromosome 1 and tgm4 gene in chromosome 8). Further investigations are required to understand their androgen-responsive mechanisms. The CA2 expression exemplifies the differential androgen dependency of the transcription between lobes, as previously reported (Harkonen et al, 1991), which showed that CA2 mRNA expression was up-regulated by androgen in the LP, whereas it was down-regulated in the DP in SD rats. In the present study, there were comparable responses in CA2 mRNA in the LP but no significant changes in the DP, which may be because of differences in androgen dosages or the mRNA quantification methods. The differential responses of CA2 to androgen suggest the lobe-specific function of this protein. Estrogen and the other hormone may be also involved in the androgen regulation of CA2 (Harkonen et al, 1991).

Recently, proteomic analysis of the human prostate and prostasomes revealed that the human prostate may secrete PRdx6 and GRP78. Another investigation searching for cancer markers found IgG Fc-binding protein expressed in the human prostate (Gazi et al, 2007). The present study shows that IgGBPLP, GRP78, and PRdx6, in addition to PSP94, TGase4, and CA2, are the aspects of secretory functionality common to mice, rats, and humans. The identified secretory proteins should be available as models of androgen-dependent gene regulation and are candidates as markers for prostatic differentiation.

Acknowledgment

We would like to thank Ms R. Tai for her expert technical assistance with the mass spectrometry.

References

Beke L, Nuytten M, Van Eynde A, Beullens M, Bollen M. The gene encoding the prostatic tumor suppressor PSP94 is a target for repression by the Polycomb group protein EZH2. *Oncogene*. 2007; 26:4590 4595.

Clements JA, Matheson BA, Wines DR, Brady JM, MacDonald RJ, Funder JW. Androgen dependence of specific kallikrein gene family members expressed in rat prostate. *J Biol Chem*. 1988;263:16132 16137.

Cunha GR, Donjacour AA, Cooke PS, Mee S, Bigsby RM, Higgins SJ, Sugimura Y. The endocrinology and developmental biology of the prostate. *Endocr Rev*. 1987;8:338 362.

Dodd JG, Sheppard PC, Matusik RJ. Characterization and cloning of rat dorsal prostate mRNAs. Androgen regulation of two closely related abundant mRNAs. *J Biol Chem*. 1983;258:10731 10737.

Donjacour AA, Rosales A, Higgins SJ, Cunha GR. Characterization of antibodies to androgen-dependent secretory proteins of the mouse dorsolateral prostate. *Endocrinology*. 1990;126:1343 1354.

Fernlund P, Granberg LB, Larsson I. Cloning of beta-microsemino-protein of the rat: a rapidly evolving mucosal surface protein. *Arch Biochem Biophys*. 1996;334:73 82.

Fischer MI, Mawson CA. Carbonic anhydrase and zinc in the prostate glands of the rat and rabbit. *Arch Biochem*. 1952;36:485 486.

Fujimoto N, Akimoto Y, Suzuki T, Kitamura S, Ohta S. Identification of prostatic-secreted proteins in mice by mass spectrometric analysis and evaluation of lobe-specific and androgen-dependent mRNA expression. *J Endocrinol*. 2006;190:793 803.

Fujimoto N, Igarashi K, Kanno J, Honda H, Inoue T. Identification of estrogen-responsive genes in the GH3 cell line by cDNA microarray analysis. *J Steroid Biochem Mol Biol*. 2004;91:121 129.

Gazi MH, He M, Cheville JC, Young CY. Downregulation of IgG Fc binding protein (FcgammaBP) in prostate cancer. *Cancer Biol Ther*. 2007;7:70 75.

Girotti M, Jones R, Emery DC, Chia W, Hall L. Structure and expression of the rat epididymal secretory protein I gene. An androgen-regulated member of the lipocalin superfamily with a rare splice donor site. *Biochem J*. 1992;281(pt 1):203 210.

Harkonen PL, Makela SI, Valve EM, Karhukorpi EK, Vaananen HK. Differential regulation of carbonic anhydrase II by androgen and estrogen in dorsal and lateral prostate of the rat. *Endocrinology*. 1991;128:3219 3227.

Heyns W. Androgen-regulated proteins in the rat ventral prostate. *Andrologia*. 1990;22(suppl 1):67 73.

Ho KC, Quarmby VE, French FS, Wilson EM. Molecular cloning of rat prostate transglutaminase complementary DNA. The major androgen-regulated protein DP1 of rat dorsal prostate and coagulating gland. *J Biol Chem*. 1992;267:12660 12667.

Imasato Y, Onita T, Moussa M, Sakai H, Chan FL, Koropatnick J, Chin JL, Xuan JW. Rodent PSP94 gene expression is more specific to the dorsolateral prostate and less sensitive to androgen ablation than probasin. *Endocrinology*. 2001;142:2138 2146.

Jones EL, Zhao MJ, Stevenson MA, Calderwood SK. The 70 kilodalton heat shock protein is an inhibitor of apoptosis in prostate cancer. *Int J Hyperthermia*. 2004;20:835 849.

Kwong J, Xuan JW, Chan PS, Ho SM, Chan FL. A comparative study of hormonal regulation of three secretory proteins (prostatic secretory protein-PSP94, probasin, and seminal vesicle secretion II) in rat lateral prostate. *Endocrinology*. 2000;141:4543 4551.

Lee C, Tsai Y, Sensibar J, Oliver L, Grayhack JT. Two-dimensional characterization of prostatic acid phosphatase, prostatic specific antigen and prostate binding protein in expressed prostatic fluid. *Prostate*. 1986;9:135 146.

MacDonald RJ, Southard-Smith EM, Kroon E. Disparate tissue-specific expression of members of the tissue kallikrein multigene family of the rat. *J Biol Chem*. 1996;271:13684 13690.

Mills JS, Needham M, Parker MG. Androgen regulated expression of a spermine binding protein gene in mouse ventral prostate. *Nucleic Acids Res*. 1987;15:7709 7724.

Naureckiene S, Sleat DE, Lackland H, Fensom A, Vanier MT, Wattiaux R, Jadot M, Lobel P. Identification of HE1 as the second gene of Niemann-Pick C disease. *Science*. 2000;290:2298 2301.

Rennie PS, Bruchovsky N, Leco KJ, Sheppard PC, McQueen SA, Cheng H, Snoek R, Hamel A, Bock ME, MacDonald BS. Characterization of two cis-acting DNA elements involved in the androgen regulation of the probasin gene. *Mol Endocrinol*. 1993;7:23 36.

Seitz J, Keppler C, Rausch U, Aumuller G. Immunohistochemistry of secretory transglutaminase from rodent prostate. *Histochemistry*. 1990;93:525 530.

Spence AM, Sheppard PC, Davie JR, Matuo Y, Nishi N, McKeehan WL, Dodd JG, Matusik RJ. Regulation of a bifunctional mRNA results in synthesis of secreted and nuclear probasin. *Proc Natl Acad Sci U S A*. 1989;86:7843 7847.

Suzuki T, Fujimoto N, Kitamura S, Ohta S. Quantitative determination of lobe specificity of mRNA expression of androgen-dependent genes in the rat prostate gland. *Endocr J*. 2007;54: 123 132.

Vercaeren I, Vanaken H, Devos A, Peeters B, Verhoeven G, Heyns W. Androgens transcriptionally regulate the expression of cystatin-related protein and the C3 component of prostatic binding protein in rat ventral prostate and lacrimal gland. *Endocrinology*. 1996;137:4713 4720.

Vercaeren I, Vanaken H, Van Dorpe J, Verhoeven G, Heyns W. Expression of cystatin-related protein and of the C3-component of prostatic-binding protein during postnatal development in the rat ventral prostate and lacrimal gland. *Cell Tissue Res*. 1998;292:115 128.

Wang MH, Grossmann ME, Young CY. Forced expression of heat-shock protein 70 increases the secretion of Hsp70 and provides protection against tumour growth. *Br J Cancer*. 2004;90:926 931.

Wang Z, Tufts R, Haleem R, Cai X. Genes regulated by androgen in the rat ventral prostate. *Proc Natl Acad Sci U S A*. 1997;94:12999 13004.

Wilhelm B, Keppler C, Henkeler A, Schilli-Westermann M, Linder D, Aumuller G, Seitz J. Identification and characterization of an IgG binding protein in the secretion of the rat coagulating gland. *Biol Chem*. 2002;383:1959 1965.

Wilhelm B, Keppler C, Hoffbauer G, Lottspeich F, Linder D, Meinhardt A, Aumuller G, Seitz J. Cytoplasmic carbonic anhydrase II of rat coagulating gland is secreted via the apocrine export mode. *J Histochem Cytochem*. 1998;46:505 511.

Wilson EM, French FS. Biochemical homology between rat dorsal prostate and coagulating gland. Purification of a major androgen-induced protein. *J Biol Chem*. 1980;255:10946 10953.

Xuan JW, Kwong J, Chan FL, Ricci M, Imasato Y, Sakai H, Fong GH, Panchal C, Chin JL. cDNA, genomic cloning, and gene expression analysis of mouse PSP94 (prostate secretory protein of 94 amino acids). *DNA Cell Biol*. 1999;18:11 26.

Environ. Sci. Technol. 2009, 43, 6611–6616

Identification of Retinoic Acid Receptor Agonists in Sewage Treatment Plants

HUAJUN ZHEN,[†] XIAOQIN WU,[†] JIANYING HU,[*,†] YANG XIAO,[†] MIN YANG,[‡] JUNJI HIROTSUJI,[§] JUN-ICHI NISHIKAWA,[∥] TSUYOSHI NAKANISHI,[⊥] AND MICHIHIKO IKE[#]

Laboratory for Earth Surface Processes, College of Urban and Environmental Sciences, Peking University, Beijing 100871, China, State Key Lab of Environmental Aquatic Chemistry, Research Center for Eco-Environmental Sciences, Chinese Academy of Sciences, Beijing 100085, China, Advanced Technology R&D Center, Mitsubishi Electric Co., 8-1-1 Tsukaguchi-Honmachi, Amagasaki, Hyogo 661-8661, Japan, Department of Pharmacology, Faculty of Pharmaceutical Sciences, Mukogawa Women's University, 11-68 Koshien Kyubancho, Nishinomiya City, Japan, Laboratory of Hygienics, Gifu Pharmaceutical University, 5-6-1 Mitahora-higashi, Gifu 502-8585, Japan, and Division of Sustainable Energy and Environmental Engineering, Graduate School of Engineering, Osaka University, 2-1 Yamadaoka, Suita, Osaka 565-0871, Japan

Received July 12, 2008. Revised manuscript received July 13, 2009. Accepted July 19, 2009.

Retinoic acid receptor (RAR) agonists are speculated to be one possible cause for the widely observed frog deformities in North America, although little is known about the specific RAR agonists in aquatic environments. We identified the specific RAR agonists in sewage treatment plants (STPs) and receiving rivers using an RAR yeast two-hybrid bioassay. Water samples were extracted by solid-phase extract cartridges, which were successively eluted by hexane, ethyl acetate, and methanol for bioassay. Among the three fractions, the ethyl acetate fraction showed the highest RAR agonistic activities. The bioassay-derived activity, expressed as all-*trans*-retinoic acid (all-*trans*-RA) equivalents (ATRA-EQ) were 10.9 ± 2.2 and 1.7 ± 1.0 ng/L in the STP influents and effluents, respectively, while the ATRA-EQs were as high as 7.1 and 8.3 ng/L in the two rivers receiving STP effluents. Following a two-step fractionation using high-performance liquid chromatography and ultra-performance liquid chromatography (UPLC) directed by the bioassay, two bioactive fractions were obtained from Gaobeidian STP influent and all-*trans*-4-oxo-RA (4.7–10.4 ng/L in influents, <0.2–0.9 ng/L in effluents) and 13-*cis*-4-oxo-RA (2.3–7.1 ng/L in influents, <0.4–1.1 ng/L in effluents) were identified in these fractions with UPLC-MS/MS. The EC_{50} for all-*trans*-4-oxo-RA or 13-*cis*-4-oxo-RA relative to that of all-*trans*-RA in exhibiting RARα agonistic activity was calculated to be 3.87 and 0.46, respectively.

Introduction

A number of papers have highlighted the potentially detrimental effects of naturally occurring and man-made chemicals on reproductive and developmental processes in wildlife and humans (*1–4*). Previous studies have paid special attention to some endocrine-disrupting chemicals which exert estrogenic activity via binding to the estrogen receptor (ER), through which the ligand–receptor complex subsequently activates transcription of target genes (*5–7*). There exist a number of nuclear hormone receptors such as the ER, androgen receptor (AR), thyroid receptor (TR), retinoic acid receptor (RAR), and vitamin D receptor (VDR), which mediate the actions of hormones and vitamins to affect processes from reproduction to development and even general metabolism (*8*). Thus, environmental pollutants binding to a wide variety of nuclear hormone receptors could induce adverse effects in wildlife (*9*), as exemplified by a recent study that organotins caused imposex in gastropods through the involvement of retinoid X receptors (RXRs) (*10*).

As one of these nuclear hormone receptors, RARs, which include three subtypes α, β, and γ, are raising the concern of environmental scientists. RARs control aspects of vision, cell differentiation, immune response, and also embryonic development in vertebrates (*11*). Ligands of RARs have been reported to be potential teratogens in developing embryos, and an agonist specific for each subtype exhibits different teratogenic patterns. RARα ligand causes deformity in the ear and mandible, and causes limb malformations, while RARβ agonist induces malformations in the liver and urinary system, and the ligand for RARγ causes ossification deficiencies and defects of the sternabrae and vertebral bodies (*12*). The natural ligands for RARs are endogenous retinoic acids (RAs) derived from retinoid (vitamin A) precursors (*13*). An excess or a deficiency of RA and related retinoids can cause abnormal morphological development, which was proven to be an RAR-mediated process (*12*). It was found that treating the larvae of Japanese flounder (*Paralichthys olivaceus*) with RA would cause deformities in the lower jaw, caudal fin, and vertebrae (*14*). Previous studies with *Xenopus laevis* have shown that exposure to RA or the RA precursor, retinyl palmitate, would induce malformations in eyes and hindlimbs (*15–18*), and similar phenomena including eye abnormalities, extra/missing limbs and/or digits have also been observed in wild frogs (*19–22*). Accordingly, the presence of RAR agonists was suggested to be one possible cause for the increasing trend of wildlife malformation (*18, 23*).

The natural RAs, which are derived from retinoid (vitamin A) precursors in humans and animals have three isomers (all-*trans*-RA, 9-*cis*-RA, and 13-*cis*-RA), and all-*trans*-RA and 13-*cis*-RA are also used in clinical treatment of dermatosis (*24*) and in cancer prevention and chemotherapy (*25*). Besides RAs, many endogenous compounds have been reported to be agonists of RARs. Some RA metabolites in humans and animals such as 4-oxo-RA, 4-hydroxy-RA, 18-hydroxy-RA, and 5,6-epoxy-RA can also bind to RARs (*26, 27*). These chemicals could be present in the environment by domestic sewage discharging and medical usage. More recently, a large number of synthetic compounds have also been proven to show RAR agonistic activity in vitro, such as organochlorine pesticides, styrene dimers, monoalkylphenols, and parabens (*28–30*). To date, few studies have investigated the occurrence

* Corresponding author phone and fax: 86-10-62765520; e-mail: hujy@urban.pku.edu.cn.
† Peking University.
‡ Chinese Academy of Sciences.
§ Mitsubishi Electric Co.
∥ Mukogawa Women's University.
⊥ Gifu Pharmaceutical University.
Osaka University.

10.1021/es9000328 CCC: $40.75
Published on Web 07/29/2009

of potential RAR agonists in aquatic environments (*23*, *31*). In a study from Canada, Alsop et al. found that methanol and dichloromethane extracts from three pulp mill effluents were able to displace more than 25% of the [^{3}H]all-*trans*-RA which bound to RARs from white sucker (*Catostomus commersoni*) gills (*31*). Gardiner et al. tested two water samples collected from Minnesota and California ponds and lakes where malformed frogs were frequently discovered, and a high response of RARα agonistic activity was detected in water samples from both places (*23*). To the best of our knowledge, however, the causative chemicals have not been identified and no paper has reported the occurrence of RAR agonistic activity in STP effluents and their receiving waters.

In this study, we determined the RAR agonistic activity in seven sewage treatment plants and their receiving rivers in Beijing, China using the RARα yeast two-hybrid bioassay. Then we identified two causative chemicals applying bioassay-directed HPLC fractionation followed by LC-MS/MS analysis.

Materials and Methods

Sample Collection. By using flow-proportional samplers, 24-h composite samples of the influents and effluents were collected each day during a one-week period (June 26 to July 2, 2006) from seven sewage treatment plants (STPs) in Beijing, China. These STPs are all operated with primary and secondary treatment processes without any post disinfection or additional filtration step. All of the plants mainly receive domestic wastewater, and detailed information on the STPs and sampling dates are summarized in Table S1 (Supporting Information). We also collected water samples by single time-point sampling from the Tonghui River and Qing River (their widths are between 15 and 25 m), which receive the effluents from Gaobeidian and Qinghe STP, respectively, in the summer (July 2, 2006) and winter (January 2, 2007). In the Tonghui River, we found two wastewater discharging pipes located at 0.55 and 2.6 km downstream, which contributed to the water flow in the Tonghui River as well as Gaobeidian STP effluent. Therefore, we set the sampling sites along the Tonghui River at 2 km upstream, and 0.5, 0.55, 2.55, and 2.6 km downstream from the discharge point of Gaobeidian STP. The sampling sites for the Qing River were located at 4 and 2 km upstream, and 2 and 4 km downstream, of the Qinghe STP. All samples were filtered and extracted within 6 h after collection. In addition, 300 mL of human urine was collected from a healthy volunteer, and a 100 mL fresh swine serum sample was purchased from National Hyclone Bio-Engineering (Lanzhou, China). Additional information about sample collection is provided in the Supporting Information.

Sample Preparation and Solid Phase Extraction (SPE) Fractionation. Water samples were filtered with a 1.2-μm pore size Whatman GF/C glass fiber pad (Maidstone, UK). After filtration, the pH of the samples was adjusted to 3.0 by adding hydrochloric acid. Oasis HLB cartridges (6 mL, Waters, USA) were conditioned by a sequence of 6 mL of hexane, 6 mL of ethyl acetate, 6 mL of methanol, and 12 mL of ultrapure water at a flow rate of 5−10 mL/min. Then 250 mL of influents, 500 mL of effluents, and 2 L of river water were extracted by passing them through 200 mg, 200 mg, and 500 mg cartridges under vacuum at a flow rate of 5−10 mL/min, respectively. The cartridges were rinsed with 10 mL of ultrapure water, and then dried under a flow of nitrogen. The dried cartridges were eluted by a sequence of 6 mL of hexane (F1), 6 mL of ethyl acetate (F2), and 6 mL of methanol (F3), respectively. The detailed sample preparation procedure is shown in Figure S1. For the influent and effluent samples, 7-day eluents of each fraction were pooled as composite samples for a complete week. Thus, 1.75 L of influent and 3.5 L of effluent from each STP were finally concentrated to 1.75 and 0.7 mL for individual fractions, respectively. Mixed eluents were prepared by combining 100 μL of each fraction to reach 300 μL in total volume. As for river water, the 2 L sample was concentrated to 400 μL for each fraction, and 100 μL of each fraction was combined to get 300 μL of mixed eluent. To determine the RAR agonistic activity of STP and river water samples, each fraction (100 μL) and the mixed sample (300 μL) were first concentrated under a gentle stream of nitrogen at room temperature, and then redissolved in 100 μL of DMSO. Finally, the concentration factors for the yeast assay of influents, effluents, and river water were 1000, 5000, and 5000, respectively. Experimental blanks were taken by extracting 2 L of ultrapure water using the same method as described above, and none of them were detected to exhibit RAR agonistic activities. The urine sample was treated using the same procedure as the water samples, and the serum sample was prepared as described in a previous study (*32*).

Two-Step Reversed-Phase Fractionation Using HPLC and UPLC. For the SPE fraction that showed RAR agonistic activity in the bioassay, a further reversed-phase HPLC fractionation was conducted. Separation was accomplished by a 4.6 mm × 250 mm symmetry shield RP18 column (Waters, Massachusetts). The column was maintained at room temperature at a flow rate of 1 mL/min. Solvent A was ultrapure water, and solvent B was acetonitrile. The gradient was started at 20% B, and was held for 3 min (0−3 min). Then the gradient was brought to 100% B in 27 min (3−30 min), and held for 10 min (30−40 min). Finally, the gradient was brought down to 20% B in 0.1 min, and this percentage was kept for 10 min (40−50 min) until the next injection. The UV detector was set at double wavelengths of 254 and 350 nm. As shown in Figure S1, 1.55 mL F2 fractions of influents, 0.5 mL F2 fractions of effluents, and 0.2 mL F2 fractions of river water samples by SPE from the seven STPs and two rivers were first concentrated under a flow of nitrogen and then fractionated by HPLC. The discrete fractions by HPLC were collected at 2-min intervals. Half of each collection was freeze-dried for yeast assay, and the other half of each collection was preserved for UPLC/MS/MS analysis. The freeze-dried collections were redissolved in 77.5 μL and 50 μL DMSO for the influent and effluent, respectively, and therefore the final concentration factors of influent and effluent were 10,000 and 25,000 for the yeast assay. For UPLC-MS/MS analysis, the collections were concentrated under a flow of nitrogen and redissolved in 60% acetonitrile solution. The final volumes for influents, effluents, and river water were 100, 100, and 50 μL, which made concentration factors of 7750, 12,500, and 10,000 for influents, effluents, and river water, respectively. The information of chemicals, UPLC-ESI-MS/MS condition, and quantitation and quality assurance/quality control (QA/QC) are provided in the Supporting Information.

For the HPLC fraction that showed RAR agonistic activity in the bioassay, ACQUITY ultra-performance liquid chromatography (Waters, Milford, MA) with great improvement of chromatographic resolution was further used for fractionation. Separation was accomplished by a Waters ACQUITY UPLC BEH C18 column (100 mm × 2.1 mm, 1.7 μm particle size). The column was maintained at 30 °C at a flow rate of 0.2 mL/min. Solvent A was 0.1% formic acid in ultrapure water, and solvent B was acetonitrile. The isocratic condition with 60% B was used for chromatographic separation. Fifty μL of the HPLC F15 fraction for influent from Gaobeidian STP, which represents 500 mL of influent, was fractionated by UPLC (Figure S1). The discrete fractions were collected at 0.5-min intervals. The collections were first freeze-dried, and then redissolved in 50 μL of DMSO for yeast assay at a concentration factor of 10,000.

Yeast Assay for RAR-mediated Activity. The yeast two-hybrid assay described in a previous paper (*33*) was applied

to evaluate the RAR-mediated activity of samples, and a detailed description is provided in the Supporting Information.

According to the guide for the derivation and application of relative potency estimates from in vitro bioassay data, multiple-point based estimates would be reasonable to characterize the potency of a variety of samples in in vitro bioassay (*34*). However, in this study, the responses for most of the STP influent and effluent samples and river water samples were less than 20% of the maximal response of all-*trans*-RA in bioassay. Thus, we evaluated the relative potency of samples and calculated the all-*trans*-RA equivalents (ATRA-EQs) based on a single-point estimation using nonlinear regression according to the dose–response curve of all-*trans*-RA developed on the same day (*34*).

Results and Discussion

RARα Agonistic Activity in Sewage Treatment Plants. Wastewater samples were extracted and eluted in three fractions, F1, F2 and F3, which represented the nonpolar, medium polar, and polar substances in the samples, and a mixed sample was reconstituted from the three fractions. The RARα agonistic activity was characterized by comparing the response magnitude caused by samples to the maximum induction by all-*trans*-RA standard at 100 nmol/L.

Of the three fractions, the F2 fraction exhibited the greatest RARα agonistic activity in both influents and effluents from all seven STP samples. In the STP influents, the magnitudes of the responses for F2 fractions ranged from 6.1% (Jiuxianqiao STP) to 21.9% (Gaobeidian STP) all-*trans*-RA Max at a concentration factor of 1000. For the effluent samples, the F2 fractions exhibited magnitudes of responses from 3.6% (Xiaohongmen STP) to 24% (Fangzhuang STP) all-*trans*-RA Max at a concentration factor of 5000. The ATRA-EQ in the F2 fractions ranged from 6.6 ng/L (Jiuxianqiao STP) to 13.4 ng/L (Wujiacun STP), and 0.9 ng/L (Jiuxianqiao STP) to 3.2 ng/L (Fangzhuang STP) for the influent and effluent samples (Table S2), respectively, which indicated that the current treatment processes can effectively remove the RARα agonists in the F2 fractions of wastewater. Among all the effluents and influents from the seven STPs, only two F1 fractions of influents exhibited weak RARα agonistic activity (Figure 1). The F1 fraction mainly contained nonpolar compounds. As for the F3 fractions, no significant RARα agonistic activities were observed in any of the samples.

For the mixed samples of three fractions, only one of the seven STP influents showed weak RARα agonistic activity, while three of the seven STP effluents exhibited relatively strong RARα agonistic activities (Figure 1). Since all F2 fractions were observed to exhibit RARα agonistic activities, this phenomenon would be explained by the presence of the matrix. Thus, the mixed samples of three fractions were spiked by 50 μg/L all-trans-RA, and the inhibition was estimated (Supporting Information) to be up to 86–103% in the influents of Fangzhuang, Beixiaohe, Jiuxianqiao, and Qinghe STPs and about 67% in the effluents except for Fangzhuang STP (97%).

RARα Agonistic Activity in Receiving River Waters. To investigate the occurrence of RAR agonists in river water due to the discharge of STP effluents, we collected water samples from the Tonghui River and Qing River, which received the effluents from Gaobeidian STP and Qinghe STP, respectively. The water samples were taken in the summer (July 2006) and winter (January 2007) from upstream and downstream of the STP discharging sites.

Similar to the results for the samples from the STPs, significant RARα agonistic activities in river water samples were observed in the F2 fractions from both the Tonghui River and Qing River (Figure 2), and their corresponding ATRA-EQ values are listed in Tables S3 and S4. It should be

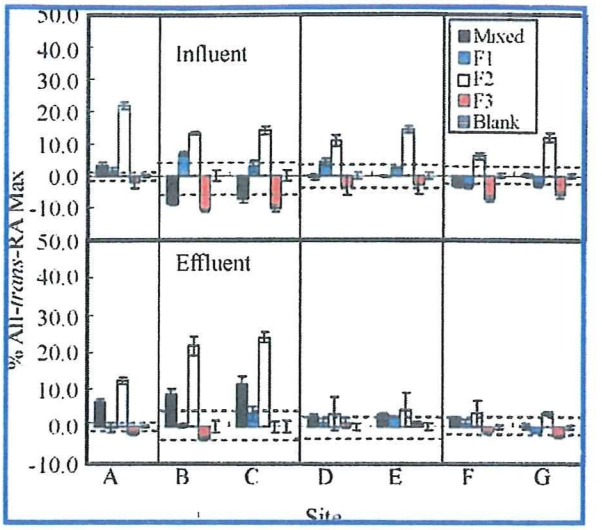

FIGURE 1. RARα agonistic activity of the influents (upper panels) and effluents (lower panels) in the seven Beijing sewage treatment plants during summer 2006. The concentration factors for influent and effluent are 1000 and 5000, respectively. Response magnitude stands for the percentage of the average maximum response observed for a 100 nmol/L all-*trans*-RA standard (% All-*trans*-RA Max). Dashed lines represent ±3 standard derivation (SD) from the mean solvent control response (set to 0% All-*trans*-RA Max): A Gaobeidian; B Beixiaohe; C Fangzhuang; D Xiaohongmen; E Wujiacun; F Jiuxianqiao; G Qinghe.

noted that two samples taken from downstream Tonghui River (0.55 and 2.6 km downstream) in both the summer and winter exhibited unexpectedly high responses of RARα agonistic activities, even higher than the activities in the corresponding STP effluents, indicating that there were other input sources in both rivers. In a previous paper reporting on the occurrence of natural and synthetic glucocorticoids at the same sites in the Tonghui River, it was also found that the concentrations of glucocorticoids were unexpectedly higher than those in the corresponding STP effluent samples (*35*). These elevated concentrations are most likely caused by a wastewater discharging pipe at the 0.55 km site (Pipe 1) which contributed greatly to the total load of glucocorticoids in downstream river. Thus, we collected the wastewater (in January 2007) from Pipe 1 (0.55 km downstream) and Pipe 2 (2.6 km downstream), and found that the F2 fractions of the samples from Pipes 1 and 2 exhibited much higher RARα agonistic activities than the river water at 0.55 and 2.6 km downstream, respectively. The ATRA-EQ in the two samples from Pipes 1 and 2 were calculated to be 67 and 94 ng/L, which were 9.4 and 11.3 times those of samples taken from the corresponding river sites, 7.1 and 8.3 ng/L, respectively (Table S3). As for the sample taken from upstream Tonghui River (2 km upstream), the RARα agonistic activities in F2 fractions were slightly higher than those from Gaobeidian STP effluents in both the summer and winter, which might be due to the undiscovered discharging sources along the upstream Tonghui River.

On the other hand, two samples from upstream (4 and 2 km upstream) of the Qing River in both summer and winter exhibited unexpectedly high responses of RARα agonistic activities. Such distribution along the Qing River is different from that of natural and synthetic glucocorticoids at the same sites in the Qing River (*35*). Considering that the glucocorticoids are originally from the discharge of humans and animals, the unexpectedly high RARα agonistic activities might be due to the discharge of other unknown sources, which needs further investigation. It is interesting that the

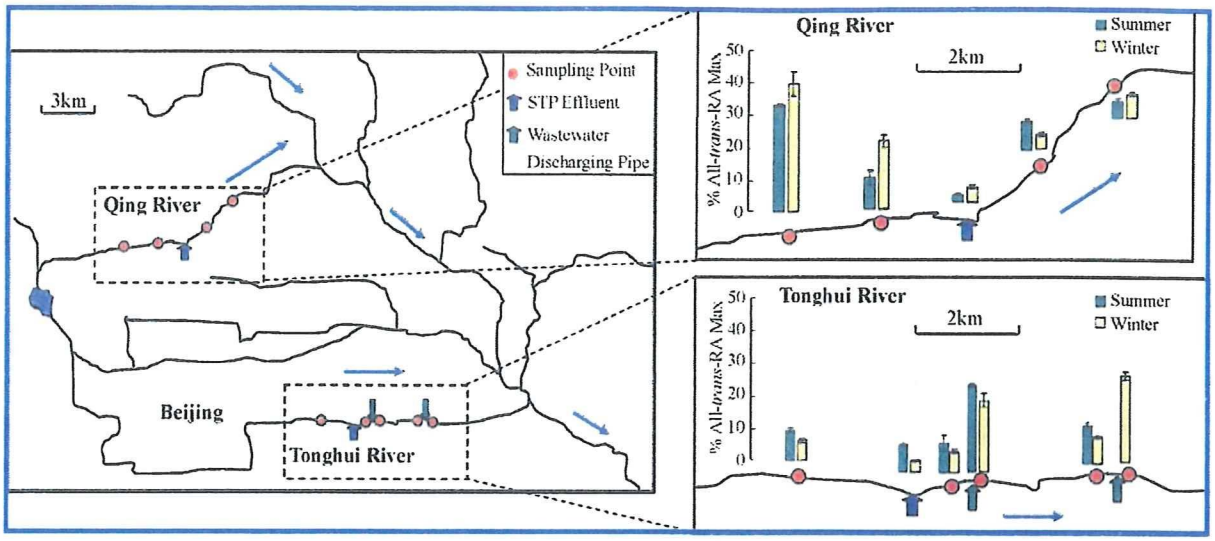

FIGURE 2. RARα agonistic activity of water samples (F2 fractions) extracted from the Tonghui River and Qing River at different distances from the corresponding STPs. The concentration factor for river water is 5000. Response magnitude stands for the percentage of the average maximum response observed for a 100 nmol/L all-*trans*-RA standard (% All-*trans*-RA Max).

two F3 samples taken from upstream sites (4 and 2 km upstream) of the Qing River in the summer caused significant responses in RARα agonistic activity tests, and this activity was comparable to that of the F2 fraction, while no detection was found in the sample taken in the winter, showing an obvious seasonal variation. However, no activity was detected in the F3 fractions of STP samples which were also taken in the summer. The reason for this difference of F3 fractions between STP and river samples is not clear, and needs to be investigated further.

Identification of RAR Agonists in Sewage Treatment Plants. As noted above, the major RARα agonists in both STP waters and river waters were present in the F2 fraction,

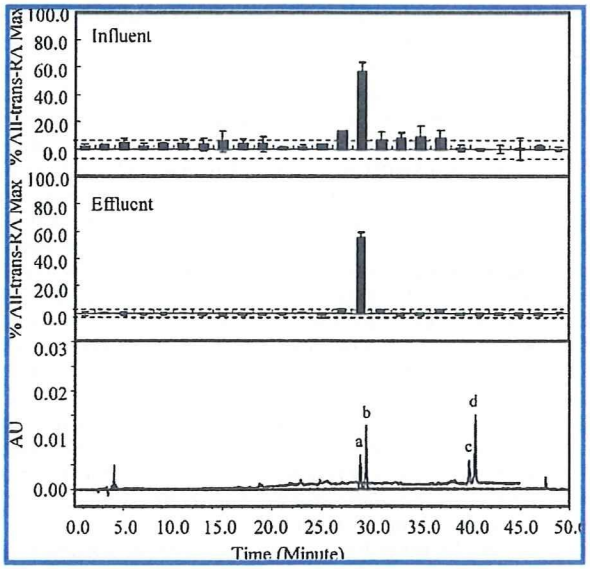

FIGURE 3. RARα agonistic activity profiles produced from F2 fractions of Gaobeidian STP influent (upper panel) and effluent (middle panel) using a bioassay-directed HPLC fractionation method. The concentration factors for influent and effluent are 10,000 and 25,000, respectively. The lower panel presents the chromatograph of several RAR agonists in HPLC with UV detector, including (a) 13-*cis*-4-oxo-RA, (b) all-*trans*-4-oxo-RA, (c) 13-*cis*-RA, and (d) all-*trans*-RA and 9-*cis*-RA. The detection wavelength is 350 nm for endogenous RAs.

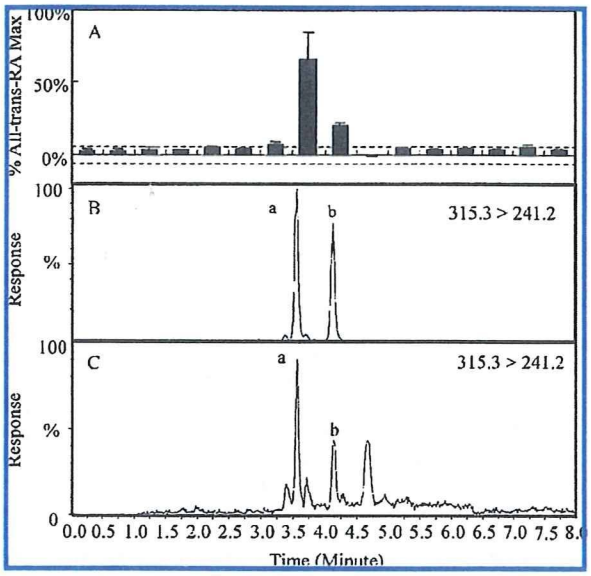

FIGURE 4. (A) RARα agonistic activity profiles of HPLC F15 fraction from Gaobeidian STP influent using bioassay-directed UPLC fractionation methods; (B) UPLC/MS/MS chromatograms of (a) all-*trans*-4-oxo-RA and (b) 13-*cis*-4-oxo-RA in mixed standards; and (C) UPLC/MS/MS chromatograms of (a) all-*trans*-4-oxo-RA and (b) 13-*cis*-4-oxo-RA in an influent sample of Gaobeidian STP.

a midpolar fraction. Thus, we further investigated the specific RAR agonists in aquatic environments using a bioassay-directed HPLC fractionation method. We fractionated F2 fractions of SPE samples from the effluents of all seven STPs and one influent, and found that the major RARα agonistic activities in all the samples occurred at the 15th fraction (HPLC F15) corresponding with a retention time between 28 and 30 min (Figure 3), indicating that this fraction is responsible for the main RARα agonistic activities in the STP samples.

To characterize the chemicals causing the response in the bioassay, we tested the RAR α, β, and γ agonistic activities of the HPLC F15 to get the phenotype of this fraction, and tried to compare the phenotype with those of already-known RAR agonists. As shown in Figure S4, both the RAR agonistic